15 Electrocoalescence for Oil–Water Separation: Fundamental Aspects

Lars E. Lundgaard, Gunnar Berg, Stian Ingebrigtsen, and Pierre Atten

CONTENTS

15.1 BACKGROUND

On the one hand electrostatic forces are special in that they may act over large distances. Effects such as lightning is one example here. This is contrary to hydrodynamic forces, which are near field forces: one mass element acts on the neighboring elements only. On the other hand, the effects of electrostatic charges and forces are significant down to a molecular level. Electrostatics therefore come into consideration in many different cases.

Electrostatics is a very important aspect of high voltage insulation design [1] where knowledge of the effects of electric fields on materials is required. Electrostatics has also found application in a number of different industrial processes, like gas filtration, separation, spraying, and copying [2,3].

Electrocoalescence is usually the denotation of an industrial separation process used on water-in-oil emulsions, where the electric fields are used to assist merging of small water drops into larger ones that will settle more quickly in a separation tank. This topic has relevance to the petroleum industry, where water-in-oil emulsions are formed by de-pressurization of oil mixed with water and also in the process of removing water deliberately added as fine emulsions in desalinizers in petroleum processing plants. The first patent for an electrocoalescer was filed in 1908 [4]. The electrostatic effects arise from the very different properties of oil and water, water having a dielectric permittivity and conductivity values much higher than those of oil (in practice one often considers water as perfectly conducting like metals).

It is the interfacial effects that stabilize water in crude oil emulsions. A vast literature exists on the chemical aspects of emulsion stability and the use of chemical de-emulsifiers [5]. Electrostatic coalescers have a potential to be an alternative to heating, which is energy consuming, and to the use of chemical emulsion breakers, which may be detrimental from an environmental viewpoint. Different voltages like dc, ac, and even pulsed dc are used for electrocoalescence, and much of the literature has focused on determining the optimum frequencies and electric field levels. Designs vary in respect to whether or not using electrode insulation, and using laminar or turbulent flows, the former one being the most popular.

To a large extent the effects of the electrostatic field are explained by body forces acting on water drops either because they are charged, giving rise to electrophoretic forces, or because they become polarized in divergent fields, resulting in so-called dielectrophoretic forces. Less attention has been paid to the phenomena occurring just when two drops are brought close to each other and eventually merge into one drop.

Without the basic understanding of the final coalescence or merging mechanism, it is not surprising that the efficiency of an electrocoalescer may vary and even disappear depending on the oil source and on the working conditions. How the design and settings should be fitted to a certain well and/or its temporal development is a crucial question. We believe that a closer look into the physical mechanisms may help overcome this type of problem.

Field-enhanced coalescence and movement of dielectric and conductive particles in an insulating environment has been studied within a number of different disciplines, and it may be useful to “take a peek over the fence” to see what is available there. The interaction of water

drops in electric dc fields has been extensively studied as an active process in cloud physics and rain formation; movement of dielectric moist cellulose particles in oil has been studied as one process responsible for triggering breakdown in transformer insulation and, finally, the behavior of suspensions of dielectric particles in oil has been investigated for applications like electrorheology.

15.2 INTRODUCTION

During the past 100 years, electrocoalescence has been used in different coalescer designs and various techniques have been promoted based on different voltage shapes, flow characteristics, and electrode shape and coating. Waterman made a survey of different applications and techniques for electrostatic treatment of water-in-oil emulsions [6]. Eow [7,8] has lately given a thorough review of the status and variations of the technique in his two papers.

Experience from oil/water separators on offshore platforms reports that coalescer efficiency often varies between wells and also with time on a given well. It is not obvious how to adapt the electrocoalescence process to the specific emulsion properties for a certain oil well. The crude oil properties will vary with respect to viscosity, conductivity, and water cut, and the interphase layer can have certain surface tension and rheological characteristics that interact with an applied electrical field: Electric forces will act on ions generated by carboxylic acids that precipitate at the interface between water and oil. Knowing that water has a permittivity of around 80 (varying from 87.9 at 0 °C to 55.5 at 100 °C) to be compared with that of crude oil (about 3), and that the conductivity values for water and oil are widely different and may vary over many decades, one cannot expect a universal optimum voltage frequency to exist for ac coalescers. It may be worthwhile to have a closer look at the role played by the components of an emulsion, particularly the influence of materials properties on the field and charge distributions under various conditions: That is to take a closer look at the basic electrostatic processes.

The aim of this chapter is to give an insight into the physical processes and properties that we know or suspect may govern the electrically enhanced and induced coalescence process of water drops in a mineral oil. Even though we do not intend to write a review of the present status of research on electrocoalescence, we will draw attention to examples from our own and other studies in this field, as well as more basic relevant background literature. We will mainly be concerned with electrostatic phenomena in stagnant emulsions and electro-hydrodynamic (EHD) phenomena, and in a limited way only consider hydrodynamic effects in the liquid bulk. Urdahl et al. [9] have given a good review of the role hydrodynamic flows play in electrocoalescence.

This chapter is organized in five parts, going from basic textbook knowledge through simpler cases concerning singular drops or drop pairs towards somewhat more speculative considerations of emulsion behavior and coalescer designs.

In Section 15.3 (Basic electrostatics) we will discuss subjects like forces between charged bodies and polarized bodies, differences between charging and conductance in metallic and dielectric bodies in electric fields, potential distribution in multi-dielectric systems and time constants for charging and charge decay of materials and systems.

In Section 15.4 we look at the forces acting on a single drop, drop pairs, and drops in an emulsion in homogeneous and inhomogeneous electric fields.

Section 15.5 explains how a drop disintegrates when stressed by an electric field and how the roles of voltage frequency and shape, surface tension, and drop size are all consistent with classic theory.

In Section 15.6 (The electrocoalescence mechanism) we discuss the validity of several different hypotheses of what really occurs in the sequence from drop proximity to established continuity

in the water phase in the two drops. Weight will be put on explaining an electric field induced surface instability being the basic coalescence mechanism.

Finally, Section 15.7 deals with practical implications and discusses how the present understanding may help in analyzing coalescer performance.

15.3 BASIC ELECTROSTATICS

15.3.1 Introduction

The characteristics and properties of dielectric materials are described with some detail in textbooks on electromagnetism. We recall only some aspects, which are of interest for the water-in-oil emulsions considered here.

15.3.2 Electrostatic Fields and Forces in Vacuum

The theory of electrostatics explains how charges create forces upon other charges and how the electric field and potential are defined.

An electric field is said to exist at a point where a stationary charge experiences a force. The electric field E is defined from the force exerted on a positive unit charge introduced at that point (see Figure 15.1). In practice we have:

$$\vec{E} = \lim_{q' \to 0} \frac{\vec{F}}{q'} \tag{15.1}$$

The limit $q' \to 0$ is required in order for the test charge not to influence the source. The simplest type of electric field, the electrostatic field, is induced by stationary charges. Two point electric charges repel each other when they are of same polarity, and attract each other when they are of opposite polarity. The interaction force follows the law experimentally determined by Coulomb. In vacuum the force between two point charges q and q' with a separation r has an inverse square law variation on r:

$$\vec{F} = \frac{qq'}{4\pi\varepsilon_0 r^2}\hat{e}_r \tag{15.2}$$

where ε_0 is the vacuum permittivity and $\hat{e}_r$ is a unit vector in the r direction. From Equations 15.1 and 15.2 the electrostatic field created by a point charge q at a point lying at the distance r

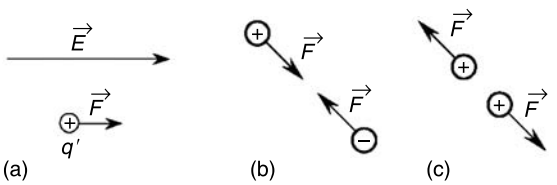

FIGURE 15.1 (a) Force on a point charge and Coulomb force between charges of opposite (b) and equal (c) polarity.

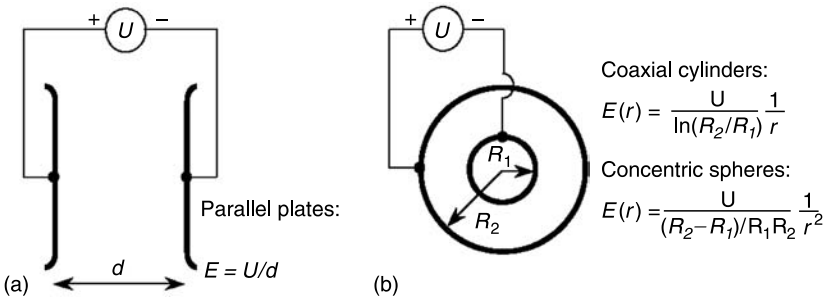

FIGURE 15.2 Examples of homogeneous (a) and inhomogeneous (b) electric field.

from q is given by:

$$\vec{E} = \frac{q}{4\pi\varepsilon_0 r^2}\hat{e}_r \tag{15.3}$$

The concept of electric field is simplest explained by looking at a planar air capacitor with two metallic electrodes of area A separated by a distance d. With a voltage U applied between the two plates one obtains a constant or *homogeneous* electric field E between them: $E = U/d$, as shown in Figure 15.2(a). This field will move free charges towards the electrodes. If one considers a point charge, this charge will induce an electric field around it that is either directed from or towards the charge. The field that decays with distance from the charge is divergent or *inhomogeneous* (Figure 15.2(b)).

The electric potential V is defined from the work done by moving a unit charge between two points in an electric field. The potential difference between two points is obtained by integrating the field along any path between these points. Potential can be defined at points and on surfaces; surfaces of metallic or other conducting materials are equipotential.

If there are many charges distributed over a volume or a surface, then the resulting field can be found by summing up the contributions from each of them. It is then easy to show that the electric field E can be expressed as the gradient of the scalar potential V:

$$\vec{E} = -\nabla V \tag{15.4}$$

The electric potential V at a distance r from a point charge is then given by Equations 15.3 and 15.4:

$$V = \frac{q}{4\pi\varepsilon_0 r} \tag{15.5}$$

If there are several charges, the resulting potential at a point is the scalar sum of the individual potentials. The electric *capacitance* of a conductor is defined as the ratio of the conductor's charge to the applied voltage, $C = Q/V$. The capacitance involves geometrical parameters.

It can further be shown that, at any point in an electrostatic field, the following relation holds:

$$\nabla \cdot \vec{E} = \rho/\varepsilon_0 \tag{15.6}$$

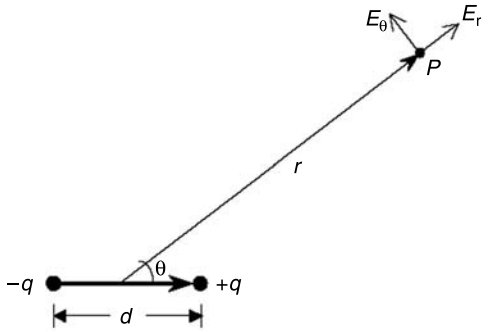

FIGURE 15.3 The electric dipole.

where ρ is the volume charge density. Combining Equations 15.4 and 15.6 leads to the Poisson equation:

$$\nabla^2 V = -\frac{\rho}{\varepsilon_0} \tag{15.7}$$

In a charge-free region ($\rho = 0$) the above expression becomes Laplace's equation. When the electrode- and equipotential surfaces coincide with the surfaces of an orthogonal coordinate system, Laplace's equation will be separable and can be solved analytically. This has been done in Figure 15.2 for rectangular (Cartesian), cylindrical, and spherical coordinates respectively.

Historically, to account for the long distance nature of electromagnetic forces, Faraday, and later Maxwell, considered the region of space occupied by an electromagnetic field to be in a state of stress, where electric (and magnetic) forces are transmitted as tension or compression by elastic lines of forces. Mathematically, this is generalized by Maxwell's stress tensor. For an isotropic medium it is easy to show that the electrostatic energy density is given by:

$$W_{\text{el}} = \frac{1}{2}\varepsilon_0 E^2 \tag{15.8}$$

An electric dipole is an arrangement of two charges $+q$ and $-q$ of opposite polarity separated by a fixed distance d; see Figure 15.3. The resulting potential from both charges at any point is given by Equation 15.5. Assuming $r \gg d$ the potential at point P will be $V = p\cos\theta/\left(4\pi\varepsilon_0 r^2\right)$, where the dipole moment is defined by $p = q \cdot d$. The radial and tangential electric field components of the dipole are found by applying Equation 15.4.

$$\begin{aligned} E_r &= \frac{2p\cos\theta}{4\pi\varepsilon_0 r^3} \\ E_\theta &= \frac{p\sin\theta}{4\pi\varepsilon_0 r^3} \end{aligned} \tag{15.9}$$

15.3.3 Polarization

Most dielectric materials, in particular liquids, are molecular compounds. An applied electric field polarizes the medium, i.e., it creates in every volume Δv a dipolar moment $\vec{p}$ proportional

to Δv: $\vec{p} = \vec{P}\Delta v$. The polarization $\vec{P}$ is generally proportional to the electric field: $\vec{P} = \chi\vec{E}$, χ being the electrical susceptibility.

In liquids there are two mechanisms generating $\vec{P}$. The first one, the electronic polarization, is universal and arises from the field induced rearrangement of the electronic clouds in the molecules. The second mechanism, orientation polarization, is specific of the so-called polar materials such that their molecules have a permanent dipole moment (it is the case of water); the field then tends to align the dipoles along its direction.

The polarization makes it necessary to define a second vector, the electric induction $\vec{D}$, in order to describe the electric state of any system with dielectric material ($\vec{D} = \varepsilon_0\vec{E}_0 + \vec{P}$). Most often the susceptibility χ is a constant scalar so that $\vec{D} = \varepsilon\vec{E}_0$, $\varepsilon = \varepsilon_0 + \chi$ being the material permittivity. Inside a dielectric material, the polarization induces an electric field that partly counteracts the field E_0 from which the polarization originates. The dielectric constant $\varepsilon_r = \varepsilon/\varepsilon_0$ gives a measure of the compensation ability.

Two charges q and q' located in a dielectric material with permittivity ε will experience a force according to the Coulomb law $F = qq'/\left(4\pi\varepsilon_0\varepsilon_r r^2\right)$. If a piece of dielectric material is placed in an electric field in vacuum, or in a lower permittivity material, the inner electric field E_i is reduced compared to the background field E_0. For a dielectric sphere this reduction is given by $E_i/E_0 = 3\varepsilon_2/(2\varepsilon_2 + \varepsilon_1)$, where ε_1 is the permittivity of the sphere and ε_2 is the permittivity of the surrounding material.

15.3.4 Conduction

Polarization inherently assumes that the material is a perfect insulator. In practice such materials do not exist. There are always some charge carriers that are free to move once an electric field is applied. Conduction properties must also be taken into account. In a metal, conduction results from movement of free electrons, while in dielectric materials it is movement of ions, electron hopping etc. In a liquid, the conduction mainly takes place through ionic movement. When an electric field E exerts a force upon an ion it will tend to move and gains an average velocity v proportional to the electric field given by its mobility K: $v = KE$. The resulting current density j is found when introducing the number of charge carriers n (assuming univalent charge carriers): $j = ne(K^+ + K^-)E$. The ability of a material to conduct current is described by its conductivity $\gamma = ne(K^+ + K^-)$, which is the inverse of its resistivity, defined by $\rho = E/j$. Ohmic conduction is defined by ρ being independent of E. Resistivity is a material parameter that, combined with geometrical dimensions of the material, gives the resistance $R = U/I$.

The conductivity in a bulk dielectric liquid is mainly governed by the ion concentration. Normally, conductivity is measured with quite low fields. In an insulating liquid (e.g., oil) conduction is ohmic only for low electric fields. Ions appear in the liquid by dissociation of traces of electrolytes dissolved in the liquid. The dissociation constant of a weak electrolyte is a function of the applied electric field according to Onsager's theory [10]. (At room temperature, the dissociation constant will increase by a factor of 10 when the electric field is increased to 5×10^4 V/cm, compared to ohmic conduction.)

Metals are different from dielectrics in that the electrons are free to move around in the conduction band. If a metal is placed in an electric field the electrons will move to the surface of the metal and arrange themselves so that the internal field in the metal is zero.

In many ways one can regard a metal as a dielectric with an infinitely high permittivity or the other way; model a high permittivity dielectric as conducting body. However, disregarding conduction in the dielectric material, even if the two cases look similar from the outside, there is an important difference: The charges on metals are free to move to another object if they get

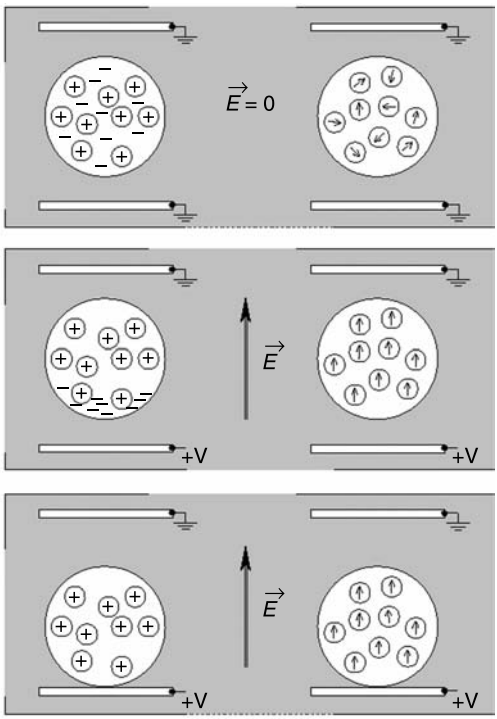

FIGURE 15.4 Polarization of conductive (left) and insulating (right) sphere and interaction with electrode upon contact. *Top*: No electric field. Evenly distributed free charges (left) and randomly oriented dipoles (right). *Middle*: Applied electric field. The conductive sphere is polarized by displacement of the free negative charges. In the dielectric sphere the dipoles try to align with the electric field lines. *Bottom*: Applied electric field, and spheres in contact with the positive electrode. Negative, free charges have moved to the positive electrode, and the conducting sphere is left with positive net charge. The dielectric sphere has no free charges and remains with zero net charge.

into contact as shown in Figure 15.4, while there are no free charges in the dielectric so it will always have zero net charge.

15.3.5 Time Constants

Conductance is the transport of free charges. From the outside it is not a priori easy to see the difference between charge movement (conductance) and charge rearrangement (polarization) within a material. In any case a charge-neutral body in an electric field will behave as a dipole. The main difference is the speed of the processes. For a metal the polarization will, for our practical cases, be instantaneous, while for dielectric bodies it will involve some time. In general, the polarization will be a quick process, compared to redistribution of charges by conduction, which takes more time.

The time constant of charge redistribution or relaxation is a material constant: $\tau = \varepsilon_0 \varepsilon_r / \gamma = \varepsilon_0 \varepsilon_r \rho$. This is equivalent to the time constant for a capacitor, $\tau = RC$, where C is the capacitance and R the internal resistance. This time constant for a material is an important parameter describing whether the material behaves like a conductor or an insulator. For time varying fields changing

much faster than the time constant the material will behave like an insulator and vice versa. Another important aspect is that charges placed in a dielectric will leak away at a rate given by this time constant.

15.3.6 Interfaces

At the interfaces between different materials continuity relations must be expressed. For two perfect dielectric materials there is continuity of the electric potential and of the normal component of electric induction:

$$\varepsilon_2(E_2)_n = \varepsilon_1(E_1)_n \tag{15.10}$$

Taking into account the conduction of the materials leads to the general relation

$$\varepsilon_2(E_2)_n - \varepsilon_1(E_1)_n = \sigma_s \tag{15.11}$$

where σ_s is the surface charge density of free charge carriers and depends on the conduction properties. When one of the materials (No. 1 here) is conducting, the field $E_1 = 0$ and the surface charge density σ_s is related to the field E_2:

$$\sigma_s = \varepsilon_2 E_2 \tag{15.12}$$

The action of the field on the surface charge density results in the so-called *electrostatic pressure*:

$$p_{es} = \frac{1}{2}\varepsilon_0 E_{\text{out}}^2 \tag{15.13}$$

15.3.7 Practical Coalescer System

The differences in dielectric properties of emulsions and of materials in electrocoalescers have several important practical implications: Both ac and dc frequencies are utilized, and one should consider the effects of the time constants on both drops in the emulsion and the emulsion itself between the electrodes.

To understand the effect of the applied voltage shape, it is important to be familiar with the terms of *capacitive* and *resistive* voltage distribution. As mentioned earlier in this chapter, the capacitance of a conductor is defined as the ratio of its charge to its potential, $C = Q/V$. As an example, we see from Equation 15.5 that the capacitance of a conducting sphere of radius R is $C_{\text{sphere}} = 4\pi\varepsilon_0\varepsilon_r R$, when the sphere is surrounded by a dielectric of dielectric constant ε_r. A typical capacitor is formed by two parallel conducting plates as shown in Figure 15.5.

The electrodes are separated by a distance d and the space between them is filled by a dielectric. When σ is the surface charge density on the plates according to Equation 15.12, the electric field between the plates is $E = \sigma/\varepsilon = (V_1 - V_2)/d$. Further, if A is the area of the plates, the capacitance of the parallel plates is

$$C = \frac{Q}{U} = \frac{\sigma A}{\Delta V} = \varepsilon_0\varepsilon_r \frac{A}{d} \tag{15.14}$$

Similarly, the resistance R between the plates is given by the conductivity γ of the dielectric, $R = d/(\gamma A)$, and the resulting charge relaxation time is $\tau = RC = \varepsilon_0\varepsilon_r/\gamma$. Under dc step

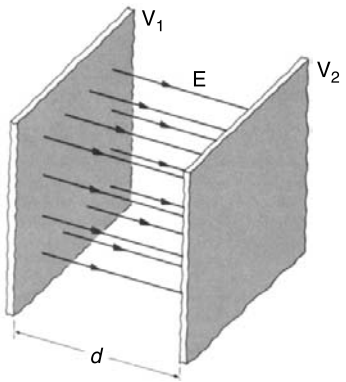

FIGURE 15.5 Parallel plate capacitor.

conditions the total current between the electrodes is the sum of a dc conduction current and a transient displacement current. The current density is expressed by

$$j = j_{\text{conduction}} + j_{\text{displacement}} = \gamma E + \frac{d}{dt}(\varepsilon E) \tag{15.15}$$

Thus, for a constant, or even slowly varying electric field, the current density and the local electric field will be determined by the conductivity of the dielectric material.

Figure 15.6 shows a simplified electrocoalescer with electrodes coated by a solid insulating material. As shown in Table 15.1, the conductivity is much lower for a solid insulating material than for a crude oil emulsion and the time constants will therefore also be very different. If a dc field is applied all ions and charge carriers will quickly move to the insulating barrier. The field distribution is governed by the conductivity of the materials and the surface charge on the solid coating. The effect of this is that the voltage drop between the metallic electrodes mainly takes place across the solid insulation; as a result there is no field in the emulsion that can activate the electrocoalescence process.

TABLE 15.1
List of Material Constants

Material	Conductivity (S/m)	Dielectric Constant	Relaxation Time Constant (s)
Solid insulation	1×10^{-16} to 1×10^{-14}	4 to 6	5.3×10^{3} to 3.5×10^{5}
Pure oil	1×10^{-13} to 1×10^{-12}	2 to 3	27 to 177
Crude oil	1×10^{-9} to 1×10^{-7}	2 to 3	2.7×10^{-4} to 1.8×10^{-2}
Purified water	$> 4 \times 10^{-6}$	20 °C: 80	1.8×10^{-4}
		90 °C: 58	1.3×10^{-4}
Water with	~ 1	20 °C: 80	7.1×10^{-10}
5 wt% NaCl		90 °C: 58	5.1×10^{-10}

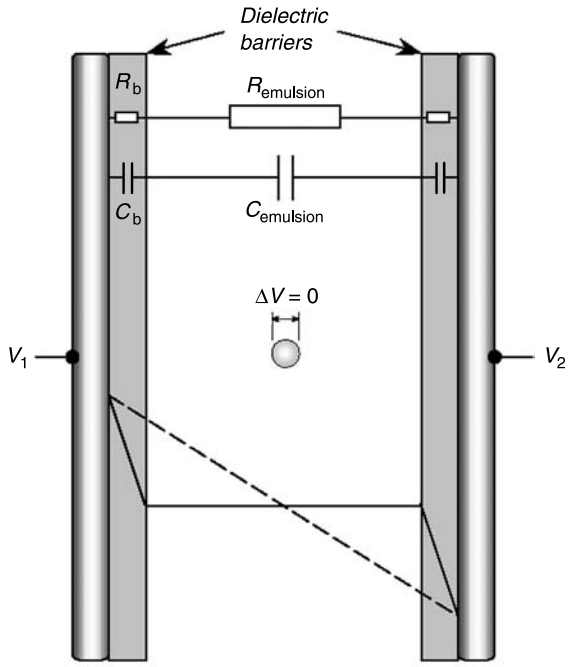

FIGURE 15.6 Example of emulsion between electrically insulated electrodes. Solid line: dc voltage distribution. Dashed line: ac voltage distribution.

If ac is applied at the system then the picture is quite different. Provided the frequency of the applied voltage has a period significantly shorter than the time constant of the emulsion, then the ions and charged particles will not have time to move to the insulating barriers and build up surface charge. It is now the permittivities that govern the electric field distribution; we say we have a capacitive field distribution.

15.3.8 Polarization and Conductivity of Water Drops

Even for highly purified water the electrolytic conductivity will be $\gamma > 4 \times 10^{-6}(\Omega\text{m})^{-1}$. When salt is added to the water the conductivity increases with the salt concentration as shown in Figure 15.7 [11]. Typically, seawater has an average salinity about 35 psu (3.5 wt% salt). The relaxation constant will be less than 1 ns, indicating that one may equal a water drop with a conductive body.

15.3.9 Processes for Charging of Drops

When a conducting body like a water drop hits a metallic plane with an electric field the particle will receive a net charge Q. For a sphere of radius a in a liquid of permittivity ε this is

$$Q = \frac{\pi^2}{6} 4\pi\varepsilon a^2 E_0 \tag{15.16}$$

The more elongated the particle is in the direction of the field the higher the charge [12].

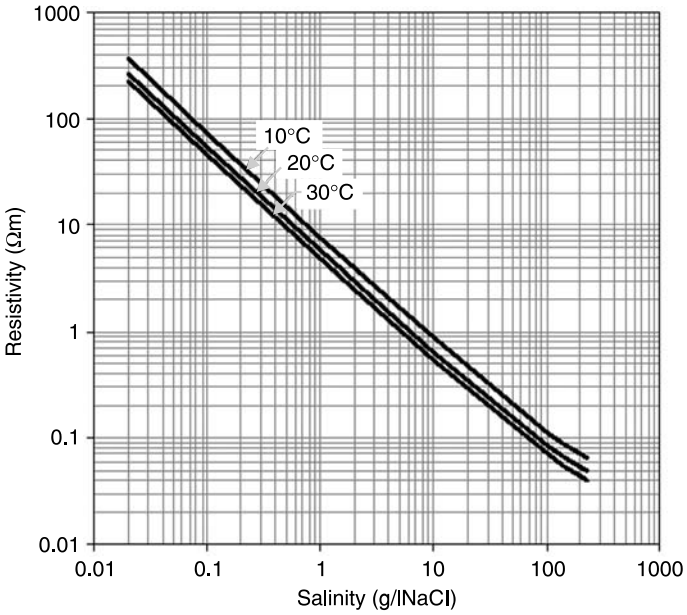

FIGURE 15.7 Resistivity of water as a function of salinity.

Water drops can also be charged in other processes such as charge transfer from other bodies, streaming electrification, adsorption of polar ions on the drop surface (preferential adsorption), and by drop breakup. The latter case is due to polarization of the water drop. As the drop is conductive, positive and negative ions will separate on the drop surfaces and provide a net charge at each drop pole. Consequently, if the drop breaks up, either by collision, turbulence, or a high field induced instability, the resulting droplets will carry net charges.

15.3.10 Chemical Surface Potentials in External Electrical Fields

So far we have considered the interface between the phases (water/oil or oil/electrode) as quite ideal, only described by its interfacial tension and a location where charges may accumulate. In reality the interface has its own microscopic electrostatic environment. Between a metallic surface and liquid there is an electrochemical potential difference; ions from the liquid accumulate at the interface and get bound to it by their electric images in the metal. At thermodynamic equilibrium ($E = 0$) this electric double layer (EDL) has a diffuse part in the liquid. The higher the number of charge carriers available, the faster the field will decrease with distance from the surface. The characteristic distance, called the Debye length, is related to fluid conductivity γ, permittivity ε, and molecular diffusion coefficient D by $\lambda_D = \sqrt{D\varepsilon/\gamma}$. As there are much more ions in water than in oil the Debye length will be much smaller in water than in oil. In aqueous electrolytes the EDL thickness has a typical value of only 1 nm. At room temperature the thermal voltage drop across this layer yields a very high internal electric field $E = (kT/q)/\lambda_D \sim 300$ kV/cm. For low conductivity oils the corresponding higher Debye length and lower internal field are respectively of the order of 5 μm and 50 V/cm [13]. With external fields of 1 kV/cm, which is in the design range for a coalescer, the diffuse layer in the oil will be swept away.

15.4 ELECTROSTATIC FORCES AND MOVEMENT

15.4.1 Electrostatic Forces Acting on a Single Droplet

Depending on the charging and polarization of a body (hereafter denoted the water drop) and the distribution of the external electric field, different forces may act. We distinguish between *electrophoretic* and *dielectrophoretic* forces. We will disregard effects from forces resulting in a change of the drop shape, assuming a fixed spherical shape.

The movement resulting from an electric field acting on a charged drop is denoted electrophoresis. As explained in Section 15.3 the force is $\vec{F} = q\vec{E}$, where the direction of the force depends on polarity of the charge q and the direction of the electric field. In the case where the particle is subjected to a homogeneous ac field the particle will oscillate, but over time no net displacement is observed. For dc fields a net movement will result. These forces do not depend on material properties. The maximum charge a drop may carry is equal to what it may acquire upon contact with an electrode (Equation 15.16). However, this charge may leak away to the surrounding oil. The time constant τ for this is given by the relaxation time constant of the surrounding liquid $\tau = \varepsilon/\gamma$, where ε is its permittivity and γ its conductivity.

Dielectrophoretic forces, on the other hand, do not require net charging, but depend on material properties. This force only arises for inhomogeneous dc or ac fields. For insulating media the direction of the force depends on the dielectric constants of the particle and the medium it is placed in. If the dielectric constant of the particle is higher than that of the surrounding medium the force will pull the particle towards higher fields (positive dielectrophoresis). If the dielectric constant of the particle is lower than for the surrounding medium the particle will be pushed away from the high field region (negative dielectrophoresis). In the case of a drop of water, which is always much more conducting than the suspending medium, the electric field inside the drop is zero and the situation is formally equivalent to a medium of infinite permittivity. Rather simplified, the positive dielectrophoresis can be illustrated by Figures 15.8 and 15.9; the drop is polarized; equal but opposite charge appears on the sides of the drop and the forces on the charge placed in the higher electric field will dominate.

The dipole moment p for a spherical particle is given by

$$p = 4\pi\varepsilon R_0^3 \beta E_0, \quad \beta = \left(\frac{\varepsilon_p - \varepsilon}{\varepsilon_p + 2\varepsilon}\right) \tag{15.17}$$

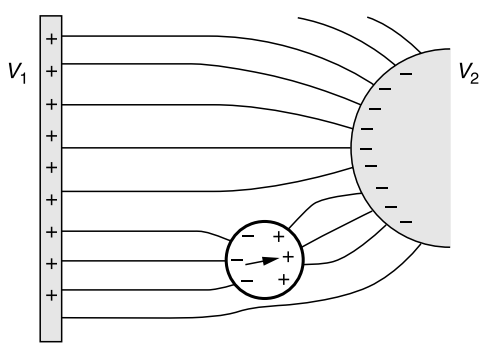

FIGURE 15.8 Dielectrophoretic forces on a water drop in oil.

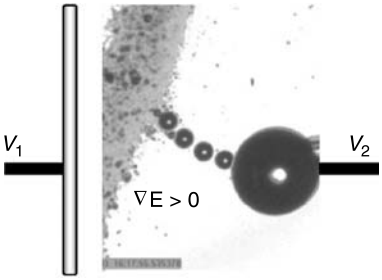

FIGURE 15.9 Experiment showing a sequence where the dielectrophoretic force attracts a water droplet out of an emulsion towards a spherical water electrode (From: A. Pedersen, E. Ilstad, A. Hysveen. Forces and movement of small water droplets in oil due to applied electric field. In: *Conf. Proc. Nordic Insulation Symposium*, NORD-IS, 2003 [14]).

where R_0 is the radius of the particle, ε_p is its permittivity, and ε is the permittivity of the surrounding medium. The dielectrophoretic force is given by the dipole moment of the particle and the gradient of the electric field: $\vec{F} = (p\nabla)\,\vec{E}$, and the resulting force becomes

$$\vec{F} = 4\pi\varepsilon R_0^3 \beta \vec{E} \nabla \vec{E} \tag{15.18}$$

For a conducting water drop, $\varepsilon_p \to \infty$, Equation 15.18 is simplified to

$$\vec{F} = 4\pi\varepsilon R_0^3 \vec{E} \nabla \vec{E} \tag{15.19}$$

For a homogeneous field $\nabla\vec{E} = 0$, and consequently $\vec{F} = 0$.

15.4.2 Mechanical Forces

In addition to the electric forces there will be forces from gravity, inertia, and from viscous effects. The buoyancy force is given by

$$F_b = (\rho_d - \rho_c)\, g V_d \tag{15.20}$$

where ρ_d and ρ_c are the densities of the drop (water) and continuous phase (oil) respectively, V_d the volume of the droplet, and g is the gravitational acceleration. In emulsions with very fine droplets (i.e., <10 μm), sedimentation is seen to be hindered by absorption of small particles on the drop surface.

For a moving droplet forces are transferred from the fluid to the droplets through friction and pressure difference. These forces are expressed exactly by the following surface integral:

$$\frac{1}{V_d}\vec{F}_{\text{fluid}} = \frac{1}{V_d}\int_{A_d} (-p_s \vec{n}_d + \tau_d \cdot \vec{n}_d) dA \tag{15.21}$$

where V_d is the volume of the droplet, A is the surface, p_s is the pressure at the droplet surface, n_d represents the unit outward normal vector, and τ_d is the shear stress tensor at the droplet surface.

The pressure and the friction on the interface are unknown and Equation 15.21 has to be modeled. In the Lagrangian framework the models for the surface integral attempt to provide particular physical meanings.

15.4.2.1 Drag Force

The "steady-state" drag force acts on a droplet in a uniform pressure field when there is no acceleration of the droplet relative to the conveying fluid. The force is given by

$$\vec{F}_d = \frac{1}{2}\rho_c C_d A\,|\vec{u} - \vec{v}|\,(\vec{u} - \vec{v}) \tag{15.22}$$

where $(\vec{u} - \vec{v})$ is the relative velocity of particle and surrounding medium. For a droplet Reynolds number Re_d below 1, the drag coefficient C_d for a rigid sphere is given by:

$$C_d = \frac{24}{\mathrm{Re}_d} \tag{15.23}$$

In fluid spheres, an internal circulation is induced that reduces the viscous part of the drag. For spherical clean bubbles and droplets, the induced internal circulation is accounted for by the Hadamard–Rybczynski equation [15]:

$$C_d = \frac{24}{\mathrm{Re}_d}\frac{\lambda + 2/3}{\lambda + 1} \tag{15.24}$$

where $\lambda = \eta_d/\eta_c$ is the viscosity ratio. In case surfactants are present surface tension gradients might appear. Le Van has suggested a model taking this into account [16,17].

15.4.3 Forces and Movement of Drop Pairs

Again we may distinguish between electrophoretic and dielectrophoretic forces. In both cases the inter-drop forces quickly fall off with distance. When drops are far from each other the forces may be neglected, at intermediate distances simple formulas based on point charges and dipole moments may be used, while when within close range charge distributions and drop geometries must be considered.

The electrophoretic force between two charged drops falls inversely with the square of the distance (Equation 15.2). The maximum charge a water drop may acquire from an electrode in a homogeneous field, disregarding drop breakup due to electric forces, can be found from Equation 15.16. Depending on polarities the force is either attractive or repulsive. These forces will only play a role in the electrocoalescence process when drops are adjacent and carry charges of opposite polarity. Furthermore, charged drops will lose their charge due to conduction through the carrying liquid.

Dielectrophoretic forces between water drops are due to the dipole moment of the drops induced by the external field. Both ac and dc fields are equally relevant. As mentioned in the previous chapter, we assume as a first approximation that the water drops are conductive spheres in an oil continuum, disregarding the conductivity of the oil. When the drops are subjected to an external field there will be induced charges on them, so that the internal field in the drop approaches zero. The charges on each hemisphere will have the same magnitude but opposite polarity. The field at each pole will be higher than the background field by a factor of 3 when the

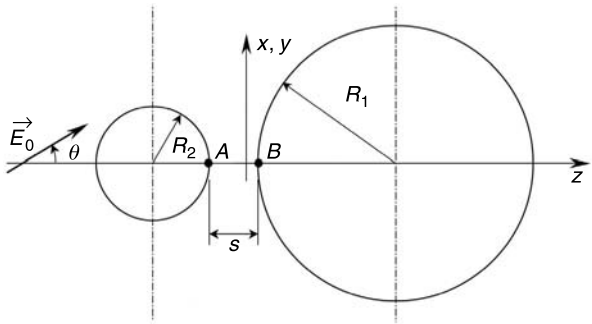

FIGURE 15.10 Two drops of different sizes located with a skew angle θ to a homogeneous electric field E_0.

drops are more than one diameter apart, see Figure 15.11. When two polarized drops get close to each other, the drops experience each other's inhomogeneous field, and they may either attract or repel each other, depending on their relative position in the external field as explained below.

Consider two drops of radii R_1 and R_2 separated by a distance s as shown in Figure 15.10. The axis between the drop centers may have a skew angle θ with respect to the applied field E_0 as indicated in the figure.

15.4.3.1 Dipole–Dipole Interaction

For large droplet distances $s/R \gg 1$ we can approximate the electrostatic interaction between two conducting droplets (the spheres are then equipotential surfaces) as the force between two dipoles located at the sphere centers. This is frequently referred to as the *point-dipole* approximation. The forces in radial direction F_r and tangential direction F_θ are [18]:

$$\begin{aligned} F_r &= 12\pi\varepsilon E_0^2 R_2^3 R_1^3 d^{-4}\left(3K_1\cos^2\theta - 1\right) \\ F_\theta &= -12\pi\varepsilon E_0^2 R_2^3 R_1^3 d^{-4} K_2 \sin 2\theta \end{aligned} \tag{15.25}$$

where d is the distance between drop centers. The coefficients K_1 and K_2 equal 1 in the point dipole approximation for the droplets.

15.4.3.2 The Dipole-Induced Dipole Model

The point-dipole approximation is not valid when the droplets are approaching each other, and the dipole moments are changed due to mutual induction between the spheres. In the literature there are different approaches to find the sphere–sphere forces beyond the point dipole approximation for multiple particles of arbitrary size and position. Clercx and Bossis [19] presented a multi-pole expansion method that gives good results, but the calculation is complex. A more promising model, the *multiple image method*, was presented by Yu et al. [20]. The first two terms in the multiple image method give the dipole-induced dipole model (DID), which is simple and numerically efficient. Siu et al. [21] show that the DID model is in good agreement with the experimental values obtained by Klingenberg et al. [18] for $s/R > 0.1$ with equally sized conductive particles. The DID model is given by Equation 15.25, with coefficients K_1 and K_2

given by

$$K_1 = 1 + \frac{R_1^3 d^5}{\left(d^2 - R_2^2\right)^4} + \frac{R_2^3 d^5}{\left(d^2 - R_1^2\right)^4} + \frac{3R_1^3 R_2^3 \left(3d^2 - R_1^2 - R_2^2\right)}{\left(d^2 - R_1^2 - R_2^2\right)^4}$$
$$K_2 = 1 + \frac{R_1^3 d^3}{2\left(d^2 - R_2^2\right)^3} + \frac{R_2^3 d^3}{2\left(d^2 - R_1^2\right)^3} + \frac{3R_1^3 R_2^3}{\left(d^2 - R_1^2 - R_2^2\right)^3} \tag{15.26}$$

In the limit $d \to \infty$ the coefficients K_1 and K_2 approach unity and we recover the point dipole expression given by Equation 15.25.

15.4.3.3 Analytical Solution

With the geometry defined in Figure 15.10 it is possible to derive analytical solutions for the potential, the electric field, and the force between the two spheres. The problem is analyzed by using bispherical coordinates [22]. Carter and Loh [23] calculated the electric field in a sphere–sphere electrode gap, with equally sized spheres. Later, Davis [24,25] gave a complete solution for the electric potential, field, and mutual forces for two arbitrary sized spheres carrying any net charge.

The maximum electric field, appearing at the drop pole A (see Figure 15.10), is conveniently written

$$E_A = E_0 \cos\theta \cdot E_3 \tag{15.27}$$

where E_0 is the background field. The field coefficient E_3 is an infinite series depending on the drop pair geometry. As shown in Figure 15.11 the electric field between the two drops increases strongly with decreasing drop distance.

The forces are found by integrating the electrostatic pressure over the drop surface. Assuming uncharged spheres the force components on sphere 2 take the simple form:

$$(F_r)_2 = 4\pi\varepsilon R_2^2 E_0^2 \left(F_1 \cos^2\theta + F_2 \sin^2\theta\right)$$
$$(F_\theta)_2 = 4\pi\varepsilon R_2^2 E_0^2 F_3 \sin 2\theta \tag{15.28}$$

where the radial force F_r can be either attractive or repulsive, depending on the angle θ, and F_θ induces a torque tending to align the drop pair with the applied electric field. The force coefficients F_1, F_2, and F_3 are complex series depending on the drop size ratio R_2/R_1 and the drop distance s/R_2. As seen from Figures 15.11 and 15.12 the electric field and the attraction force increases rapidly with decreasing drop distance.

Unfortunately, the computational cost required for calculating F_1, F_2, and F_3 is high in a multi-droplet situation. However, the exact solution is excellent for benchmarking other models in cases with two particles/droplets. The different approximations are compared in Figure 15.13. For large drop separations $s/R_2 \gg 1$ the force coefficients F_1, F_2, and F_3 approach the values of the point-dipole equation (15.25).

For small separations $s/R_2 < 1$, F_2 and F_3 take constant values while F_1 diverges. Atten [26] proposed the following empirical asymptotic expression, valid in the range $10^{-3} \le s/R_0 \le 10^{-1}$:

$$F_1 = 1.25/(1 + (R_2/2R_1))^4 \, (R_2/s)^{0.8} \tag{15.29}$$

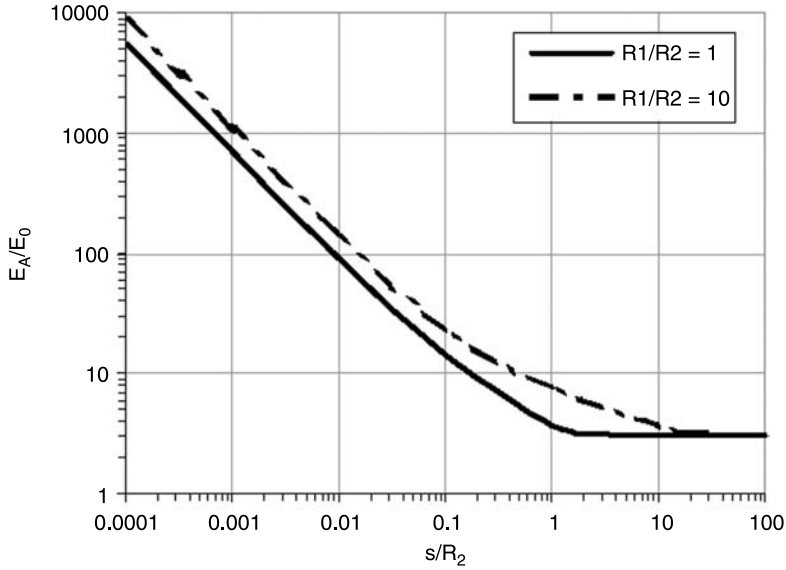

FIGURE 15.11 Electric field enhancement at the pole A as a function of the reduced drop pair distance s/R_2. The electric field E_0 is parallel to the drop axis.

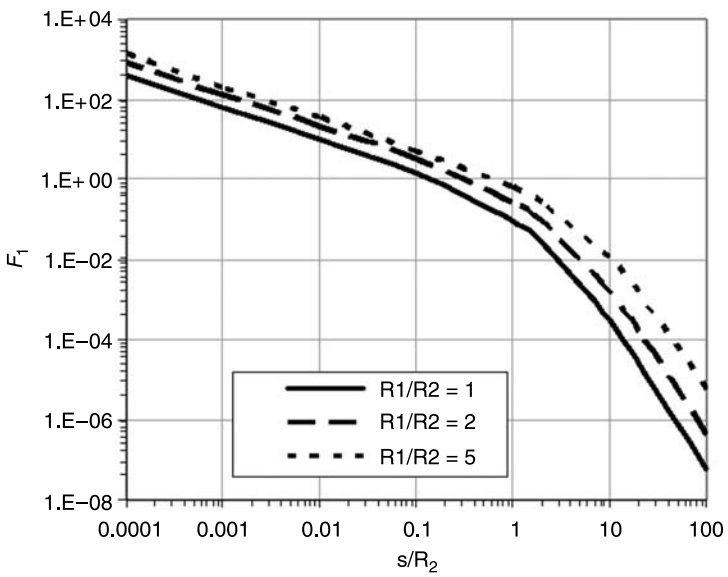

FIGURE 15.12 Force coefficient F_1 as a function of the reduced distance s/R_2 for different drop size ratios.

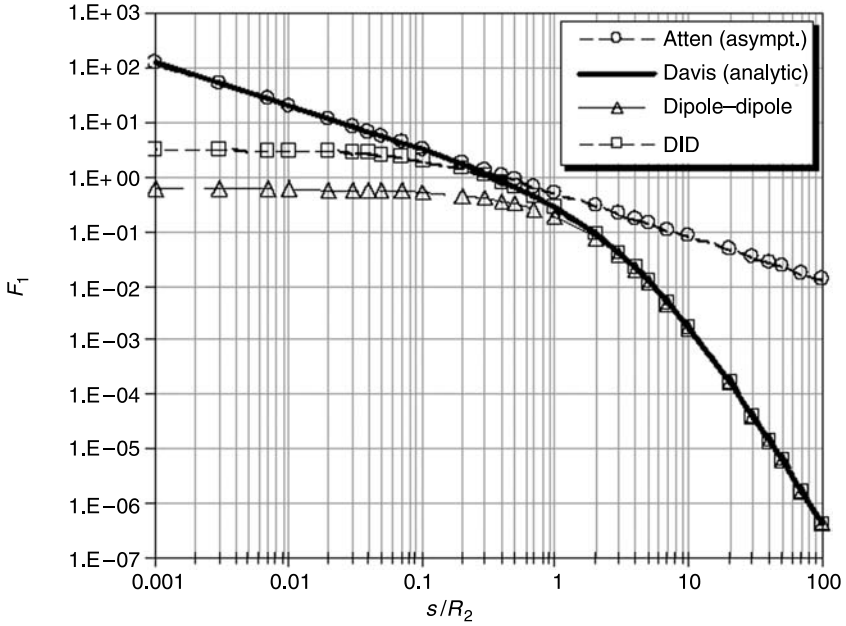

FIGURE 15.13 Comparison of different models for the attraction force between two conducting droplets. The drops are aligned with the electric field ($\theta = 0$). Drop size ratio $R_1/R_2 = 2$.

In the particular case of spheres of equal radius R_0 aligned with the field ($\theta = 0$), Williams [27] derived asymptotic relations for the potential difference between the two spheres:

$$\Delta V = \frac{2\pi^2}{3} \frac{E_0 R_0}{\log\left(\dfrac{R_0}{s}\right)} \tag{15.30}$$

and the electric field at the facing poles:

$$E_{\text{pole}} \cong \frac{2\pi^2}{3} E_0 \frac{R_0/s}{\log\left(R_0/s\right)} \tag{15.31}$$

The attraction force then takes the expression:

$$F_r = \frac{2\pi^5}{9} \varepsilon E_0^2 R_0^2 \frac{R_0/s}{[\log\left(R_0/s\right)]^2} \tag{15.32}$$

For drops with a separation of one drop radii or more it is easy to show from Equation 15.25 that the resulting force is repulsive, $F_r < 0$ when $3\cos^2\theta < 1$, that is, when the angle θ between the drop pair and the electric field exceeds 54.7°. Now this does not hold for drops with small separation. In the case of very small separation the angle approaches $\pi/2$, which can be found from Equation 15.28, implying that close drops nearly always attract each other. This analysis is done for a static case, disregarding the influence of hydrodynamic forces. Experiments done by

Pedersen [28] with drop pairs moving in stagnant liquid due to buoyancy and dielectrophoresis in a 50 Hz field confirm the transition from repulsive to attractive force at 55°. However, drops that were expected to repel each other quickly shifted position and then aligned with the electric field. These observations can be explained by the hydrodynamic drag from one particle influencing the other.

The above expressions are valid only for spheres. At high fields the electrostatic pressure on the drop surface tends to stretch a drop to a nearly ellipsoid shape. When two drops are close the deviation from a spherical shape will be most significant on the surface of the larger drop, in the direction of the smaller drop. This is due to the lower hydrostatic pressure inside the largest drop. However, with practical electric fields and drop sizes the deformation will only be of importance when $s/R_2 \ll 1$ [29,30].

15.4.3.4 Film-Thinning Force

The film-thinning force is caused by drainage of the liquid film between two approaching droplets. The derivation of the formulas usually requires that the gap between the particles is small, $s \ll a$, and that the flow is within Stokes regime $\mathrm{Re}_d \cdot s \ll a$, where $a = (R_1 R_2)/(R_1 + R_2)$ is the reduced radius. The film-thinning force is written as [31]

$$\vec{F}_f = \frac{-6\pi \mu_c a^2 (\vec{v}_r \cdot \vec{e}_r)}{s} f^* \vec{e}_r \tag{15.33}$$

where $\vec{v}_r$ is the two drop relative velocity and $\vec{e}_r$ indicates the direction of the relative motion. In the case of rigid sphere the function $f^* = 1$. For very close liquid spheres expressions compensating for proximity effects have been developed by Vinogradova [32] and Barnocky et al. [33].

15.4.4 Electrostatic Models for Multiple Spheres

When more than two spheres are considered, Laplace's equation can only be solved numerically. This is possible with a fast computer code; but with increasing number of spheres the calculation time can be quite considerable. Faster calculations are obtained by using the method of images or multipole expansion [34–41]. These methods are applicable to both dielectric and conductive particles. As mentioned in the previous sections, the electric field of a conducting sphere can be exactly represented by a dipole p or a point charge Q at the sphere center. Two spheres could be modeled, to a first order approximation, by two point charges or two dipoles at a distance s located at the respective sphere centers. However, due to the mutual induction between the charges or dipoles, the corresponding spheres will no longer be equipotential surfaces. This is corrected by recursively adding more charges Q' or dipoles p' at increasing distance from the sphere centers. The major advantage with these methods is that the force exerted on one sphere by the other is simply found by summing the forces between all electric images (Coulomb's law). Further, the polar interactions in a multiparticle system are pairwise additive. Inspired by the work by Jones [37], Bosch [42] developed a simpler method using dipole images to calculate the force between two conducting spheres in an external electric field. The results fit well to the previous results by Davis [25], and according to the author the method can readily be extended

to more than two spheres. This method is effective as it uses a simple matrix inversion rather than numerous charge/dipole iterations.

15.4.5 Forces and Movement in Emulsions

For a water-in-oil emulsion the case is more difficult as analytic expressions are not readily available. The two main questions are: What is the local electric field?, and, How can forces between multiple bodies be calculated?

If the distribution of the emulsion is inhomogeneous the background field may be influenced; increasing in the regions with the lower water cut. This may be explained by the fact that when two dielectric materials are put in series in an electric field, the stress increases in the lower permittivity dielectric due to polarization effects. An emulsion with a high water cut will have higher permittivity than one with a low water cut due to the effect from the high permittivity and conductivity of water.

We expect that for emulsions with a water cut below 5% it is possible to use the formulas for fields and forces presented in this section, because only rarely are more than two drops at a time within near-field distance of each other (i.e., within one drop radius distance; see Figure 15.13). This allows simulations based on discrete element method (DEM) code [43].

The topic of multiple particle ($n > 2$) interaction in a flowing dielectric liquid is thoroughly treated in the field of electrorheology, and will not be discussed further here. See for instance Refs. 18–21,34,44–47.

Some experiments were carried out on stagnant emulsions to get a preliminary impression of the behavior of such a complicated system. The amplitude, frequency, and waveform (square/sine) of the applied voltage were varied. The experiments were similar to what was previously reported [48]; a drop of fine water-in-oil emulsion (diameters below 10 μm) was injected into a pure oil phase in a homogeneous electric field between two electrodes.

In the experiments it was impossible to avoid charged drops due to the tribo-electric effects during processing of the emulsion. The bulk fluid had a very low conductivity giving a charge relaxation time of several minutes. The effect of charged droplets seemed to influence the electrocoalescence for all emulsions. Generally, for frequencies below ~100 Hz the movement of the majority of drops was dominated by the electrostatic alternating forces on the droplets being electrically charged. Charged droplets were either resident or obtained from drops touching each other and exchanging charge before separating again. Charges were easily scattered across the emulsion due to the drop–drop interactions. The resulting oscillating movement of the bulk oil lowered the electrocoalescence efficiency. For higher applied frequencies, above ~300 Hz, electrostatic movements of charged drops were locally confined and less influencing the surrounding emulsion. In general, coalescence efficiency decreased with decreasing emulsion average drop size and water cut, and there was no clear observable effect on the efficiency of the coalescence from the voltage shapes. The presence of a larger drop, as shown in Figure 15.14, increased the coalescence rate strongly by "sucking up" small droplets from the emulsion.

Water-in-oil emulsions without chemical stabilizers added, with 10 to 20 μm initial drop size and water cuts up to 20%, showed no field induced coalescence. Chemically stabilized emulsions with even smaller drop sizes (1 to 10 μm diameter) behaved differently. These stabilized emulsions, being vastly denser, showed a highly active electrocoalescence. Furthermore, for the case of the denser chemically stabilized emulsions, we observed an unexpected sudden and continuous expansion of the emulsion volume during some time (and voltage periods) starting at application of the electric field. The phenomenon was promoted by high electric fields, suppressed by an increasing voltage frequency, and most intense using bipolar square voltages. The expansion

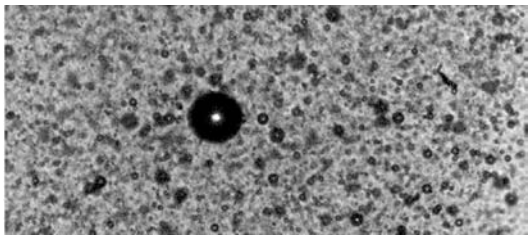

FIGURE 15.14 Picture from emulsion experiments in a horizontal electric field, showing a large drop sucking up small droplets from the emulsion.

FIGURE 15.15 Chain formation in a stagnant liquid. Square wave voltage, 3.5 kV/cm horizontal electric field.

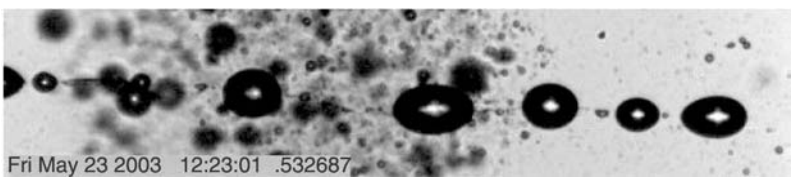

FIGURE 15.16 Chain formation along the horizontal electric field. Small, stable droplets in the chain tend to obstruct coalescence.

continued until the emulsion volume had reached a new and lower density. The higher optimum frequencies preserved emulsion density and therefore coalescence efficiency. For increasing frequencies up to 10 kHz the chain formation became less pronounced as the coalescence efficiency increased.

Very often droplets formed chains that were aligned with the electric field; see Figure 15.15. These drops grew larger in time as chains coalesced internally, and more drops were added to the ends of the chains. Often, the coalescence rate for chains of larger droplets (>100 μm) was lower

than theoretically expected, apparently due to intervening particles and very small, stable water droplets as seen in Figure 15.16. The droplet chain formation seemed a natural and significant part of the multi-droplet electrocoalescence.

15.5 DROP INSTABILITIES

So far we have treated the water drops as rigid spheres. However, when an electric field is applied on a soft conductive body like a water drop, it will change its shape, become elongated, and in the end may break up due to electric field forces [49]. This is explained by the classic theory by Taylor [50] developed for water drops in dc fields. We have studied the phenomenon for water drops in oil under various voltage shapes and frequencies, and found good agreement with classic theory. However, classical theory only considers an ideal interface between oil and water only characterized by its interfacial tension. In reality the interface has not a zero thickness, and we expect that for real emulsions surface rheology will play a role introducing new time constants and gradients in the surface characteristics (such as the Marangoni effect known from chemistry).

15.5.1 Classical Theory of Drop Instabilities

In the absence of an electric field the interfacial tension T will keep the water drop spherical with radius r when the gravitational effects are negligible (Bond number $Bo = \Delta\rho g r^2/T \ll 1$). The pressure difference across the interface of a drop of radius r due to surface tension is then $\Delta p = 2T/r$. The shape stability is therefore higher for smaller drops.

When a uniform field is applied, the drop will deform due to the electric stress on the surface, and the drop will elongate in the direction of the electric field. There are two different classical approaches to model the elongation of the drop. Both models assume that the drop takes the shape of a prolate spheroid. Sherwood [51] used an energy argument, where the drop takes a shape that minimizes the total energy, which is the sum of the electrostatic and surface energy. In this model it is possible to vary the permittivity and conductivity of the drop liquid and of the suspending fluid. Taylor [49,50] used a simpler approach, seeking for a static solution such that the pressure difference across the drop interface is the same at any point on the surface. This pressure difference is due to the effect of interfacial tension and electrostatic pressure. Postulating that the shape of the deformed drop is an ellipsoid, it is sufficient to estimate Δp at two points, at the drop pole and at the equator. Balancing the two pressure differences, $\Delta p_{\text{pole}} = \Delta p_{\text{eq}}$, gives:

$$E_0\sqrt{\frac{2r_0\varepsilon}{T}} = 2\cdot\left(\frac{b}{a}\right)^{\frac{4}{3}}\left(2-\frac{b}{a}-\left(\frac{b}{a}\right)^3\right)^{\frac{1}{2}} I_2 \tag{15.34}$$

where

$$I_2 = \frac{1}{2}e^{-3}\ln\left(\frac{1+e}{1-e}\right) - e^{-2} \tag{15.35}$$

where e is the eccentricity defined by $e = \sqrt{1-b^2/a^2}$, and a, b are the semi-axes of the prolate spheroid. The drop elongation as a function of the applied electric field is plotted in Figure 15.17.

The drop elongation increases with the field up to a limiting aspect ratio above which the droplet becomes unstable. The corresponding field is called the critical field E_c. Considering the special case of a fully conductive droplet, Taylor [50] showed that a stationary prolate spheroid

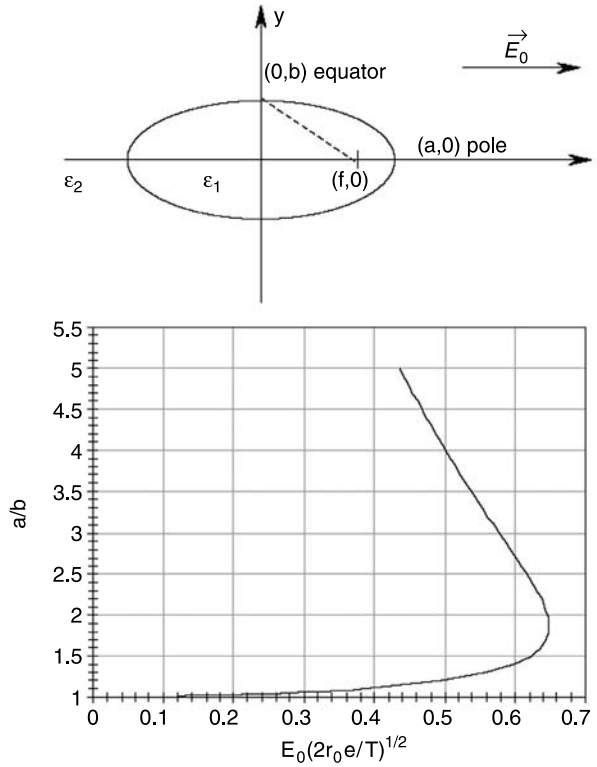

FIGURE 15.17 Theoretical elongation of a water drop as a function of the applied electric field. *a* is the long semi-axis and *b* is the short one.

has a maximum possible aspect ratio $a/b \cong 1.9$, as shown in Figure 15.17. At this maximum value of a/b the applied field E_o equals the critical field E_c, found to be:

$$E_c = 0.648\sqrt{\frac{T}{2\varepsilon r_0}} \tag{15.36}$$

At higher values of the applied field E_o the drop becomes unstable at the poles and breaks up. This model fits well to experimental data for dc and low frequency alternating voltages. More accurate expressions for the critical field can be found in Ref. 52.

15.5.2 Experimental Observations of Disintegration of Water Drops in Oil

A study of instabilities of sub-millimeter water drops in refined naphthenic oil was performed varying the frequency and the shape of the applied ac voltage [53]. The drops were slowly falling by gravity in a horizontal electric field while the voltage was gradually increased. A camera was used to observe the changes in shape and to determine in what conditions the instability occurs.

For dc voltage it was difficult to keep the drop in the field of view as it easily got charged and was pulled toward an electrode. The frequency of applied ac voltage was varied from 2 Hz to 2000 Hz. When increasing the voltage amplitude, the droplets deformed into prolate spheroids

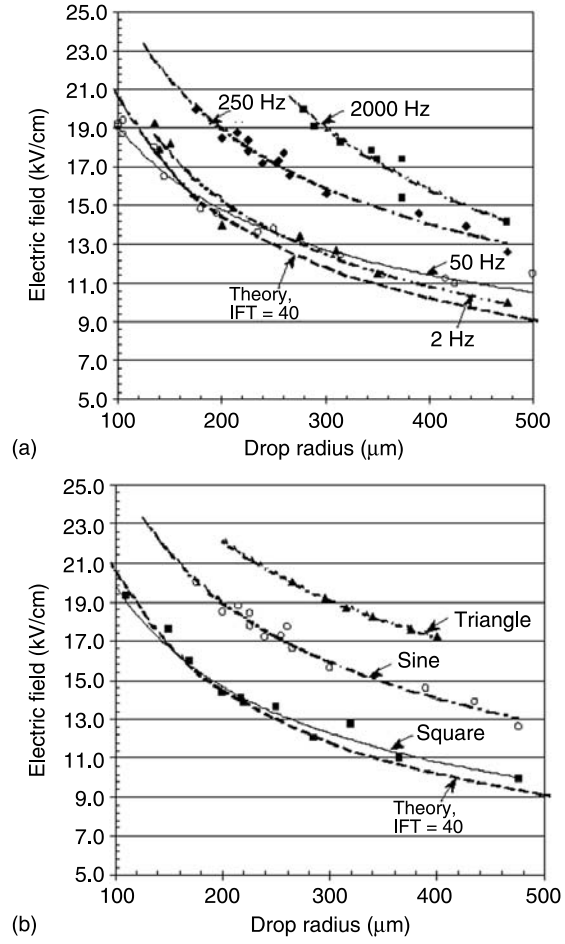

FIGURE 15.18 Drop breakup field strength for (a) varying frequencies of a pure sine voltage and (b) different shapes of applied voltage at 250 Hz.

pulsating at twice the voltage frequency as expected. For low frequencies in the range 2 to 50 Hz the measured critical field for drop disintegration is in very good agreement with the theoretical values obtained from Equation 15.36, independently of the voltage waveform. At higher frequencies, however, the critical field increases with the applied frequency as shown in Figure 15.18(a).

The different voltage waveforms used in this study were triangular, sinusoidal, or square. For frequencies above ~100 Hz the observed critical field was also depending on the voltage waveform when the frequency was kept constant, as shown in Figure 15.18(b).

The disintegration of water droplets is well predicted by theory for low applied frequencies, independently of the voltage waveform. However, at increasing frequencies, a stronger field is required to reach the drop instability. This can be understood taking into account the inertia of the system. For very low frequency, the drop deformation follows the changes in electrostatic pressure so that, despite the oscillating character, at every moment the drop is in quasi-static equilibrium.

Instability then occurs when the maximum field value takes the critical expression (15.36). Raising the frequency makes the inertia effects grow; when inertia forces become of the same order as the capillary and electric forces, the amplitude of drop oscillation decreases and a higher field is required to reach the critical elongation a/b. At high frequencies, the oscillation amplitude is very small and can be disregarded; then instability sets in when the effective field takes the critical value E_c. Therefore we expect a ratio $\sqrt{2}$ between high and low frequency critical values of the effective field for sine waveform and $\sqrt{3}$ for triangular waveform. This justifies the observations that $E_C^{\text{square}} < E_C^{\text{sine}} < E_C^{\text{triangle}}$ at a given high frequency. Furthermore, results of Figure 15.18 are in reasonable agreement with these estimates.

Increasing the conductivity of the water phase did not induce any noticeable effect on the critical field strength. This is expected, due to the huge difference in conductivity of water and oil. The influence of surface characteristics was also investigated by adding asphaltenes. Adding these compounds leads to a decrease in the stability of the water drops in an electric field, presumably due to the lowering of the interfacial tension.

Very likely the above considerations about the effect of inertia are only part of the story. Strictly speaking, Equation 15.36 gives the highest field strength for which a static deformation of the drop can exist. This implicitly corresponds to a dc applied field (a square waveform ac field practically provides a constant electrostatic pressure). A detailed instability analysis is necessary in the case of ac applied field of sine or triangular waveform to account for the influence of frequency. The frequency and waveform of the voltage should play a role in the development of the pointed ends of the drops and the subsequent formation of a thin jet or ejection of small droplets. The observed drop disintegration is not always like the Taylor cone-jet formation shown in Figure 15.19, which assumes stationary (dc) conditions.

At instability the deformation and eventually disintegration depended on the ac frequency and shape. We could see that the behavior around the critical voltage was nonstationary; at lower frequencies dominated by pulsation of the droplet. During this dynamic situation, aspect ratios far exceeding the theoretical 1.9 from the stationary situation were observed. Several factors will play a role: Ejection of mass from the ends of the drop involves loss of charge, viscosity, and drop sizes etc.

Different instabilities from the pointed ends of the droplet were observed, involving ejection of drops of various sizes from large droplets to very fine clouds, as shown in Figure 15.20.

Once the instability has started it will continue until the original drop size is reduced below the critical limit. In our experiments the instability usually ended with a violent final breakup, observed in different modes like separation into a few droplets (sometimes by a sausage instability) or a more explosion-like event.

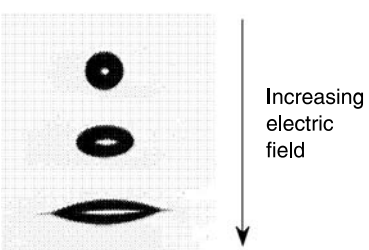

FIGURE 15.19 Drop stretching and Taylor cone formation with thin jet instability during increasing field.

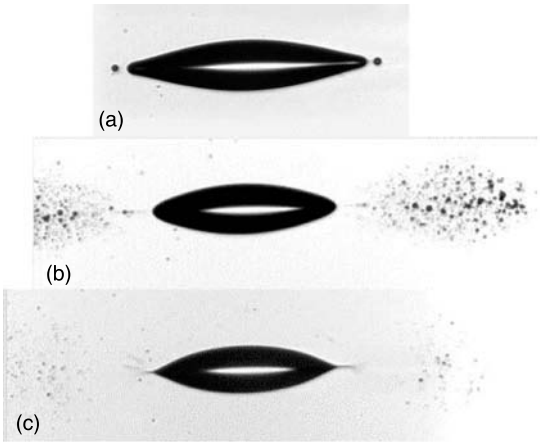

FIGURE 15.20 Observed instability types: (a) ejection of single droplets, (b) ejection of cloud of droplets, and (c) ejection of cloud of fine droplets.

15.5.3 Dynamic Study of Drop Shape for Transient Electric Fields

The resonance modes $n \geq 2$ for a free drop have been calculated theoretically [54] for water drops in air. For a water drop in a dielectric liquid the $n = 2$ mode dominates, as the drop surface dynamics is damped by viscous effects. The transient oscillations of a drop elongating to a steady state spheroid can be studied by applying a short square wave voltage pulse. In the same way, the relaxation of the drop surface can be observed when the voltage is turned off. This can be used to measure the surface elasticity and other dynamical properties of the water/oil interface, such as the time constant of surfactant absorption. The drop surface elasticity e follows the definition given by Gibbs [55,56]

$$e = \frac{dT}{d \ln A} \tag{15.37}$$

where T is the interfacial tension and A is the surface area of the drop. Figure 15.21 shows as a typical example the transient evolution of a water drop in a liquid without surfactants, while Figure 15.22 shows the damping effect when the drop surface is saturated by asphaltenes.

This significantly damped dynamic behavior affects the instability formation, which is slowed down by the less flexible drop surface. Water drops with asphaltene saturated surfaces would frequently exhibit a stationary elongation of more than twice the theoretical break-up value $a/b = 1.9$.

15.6 THE ELECTROCOALESCENCE MECHANISM

From Sections 15.4 and 15.5 we obtain a picture of an applied electric field that induces attractive forces between close drops: it brings pairs of drops closer until they eventually coalesce. This picture applies for stagnant emulsions but not strictly in the case of electrocoalescers in which the suspending oil is in motion. For an emulsion characterized by a laminar or turbulent flow, due to the action of shear, the drops in a volume around a particular drop have a relative motion,

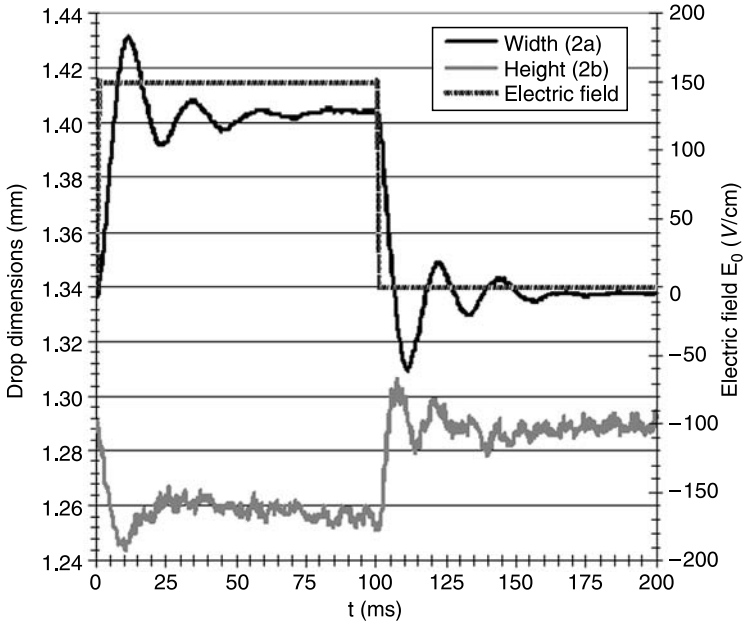

FIGURE 15.21 Transient oscillations of a 1.34 mm diameter water drop in paraffinic oil Exxsol D80.

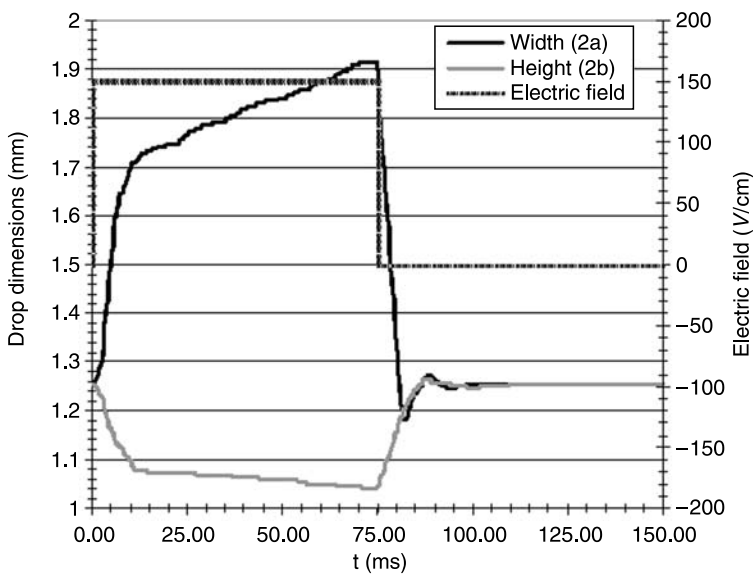

FIGURE 15.22 Transient deformation of a 1.25 mm diameter water drop in naphthenic oil with 100 ppm (wt) asphaltenes dissolved. Measurements after 155 min saturation time.

which can bring some of them in close vicinity at some moments. In the separators not applying electric fields, these quasi-collisions of drops result in pairs of drops rolling off each other during some time. Without an electric field the rate of natural coalescence for adjacent drops is very low. In the presence of an applied electric field, the rate of coalescence is much higher and increases with the field magnitude. We can thus distinguish two stages in the electrocoalescence process, the first one that brings two drops in close vicinity (and which is determined mainly by the flow), and the second one in which the electric field promotes their coalescence [26].

In this section we focus on the second stage, i.e., on the coalescence of two close drops under the action of an electric field. This is a rather complex situation and we consider here the simplest possible case by assuming that:

- The water droplets are electrically neutral (no net charge).
- The water is assumed to be perfectly conducting and the suspending oil perfectly insulating.
- The two droplets are identical and their centers are aligned with the electric field.

Moreover, the following considerations implicitly assume that the drops have a small radius and that the distance between their facing interfaces is smaller than their radius.

15.6.1 Merger of Drop Pairs

The main question that arises concerns the nature of the mechanism resulting in the final merging of two very close drops; this is important for practical applications because a good knowledge of this mechanism could help to augment or hinder electrocoalescence. Three main scenarios may be proposed:

- The field strength between the water drops is high enough to initiate an electric discharge and a shock wave that punctures the oil film.
- The attraction force between the drops brings them closer and closer and coalescence takes place at the end of the process of thinning of the oil film separating them.
- The electrostatic pressure induces a deformation of the water–oil interfaces and coalescence arises for a finite value of the drop separation when at least one of these interfaces becomes unstable.

The possibility of getting partial discharges between water drops was suggested by Lundgaard and colleagues [48]. However, such a mechanism for triggering coalescence appears very unlikely. For drops of diameter exceeding, typically, a millimeter, the electric field should induce their disintegration and not a discharge. For droplets of diameter $2R_0 < 100$ μm (which is the case for emulsions treated by electrocoalescers), electrical discharges between close droplets appear impossible. Indeed, similarly to the case of gases, there is a minimum required potential difference for electron avalanches in the oil phase. Now from the results given in Section 15.4, the potential difference ΔV between two electrically neutral drops is lower than the product of the field E_0 (applied to the emulsion) and the distance between drop centers. For close identical droplets this gives $\Delta V < 2R_0E_0$. With a background field $E_0 = 1$ kV/mm (being a high field in a coalescer), we obtain $\Delta V < 100$ V, a value lower than the minimum Paschen voltage for self-sustained discharge in the suspending oil. Therefore in electrocoalescers used to augment the size of water droplets of the water-in-oil emulsions, the coalescence cannot be triggered by electrical discharge between droplets.

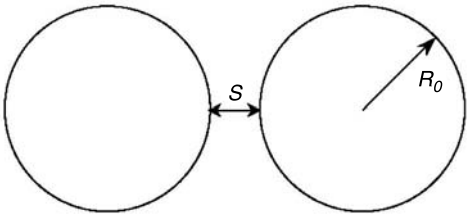

FIGURE 15.23 Two conducting spheres at distance s.

In conventional coalescence models, film drainage between drops plays an important role as a barrier to overcome to get the drops in contact [57]. For two undistorted spheres of radius R_0 at a small distance s (see Figure 15.23) the law for film thinning deduced from Ref. 32, and which is also given by Allan and Mason [58], is:

$$\frac{ds}{dt} = -\frac{2Fs}{3\pi\eta R_0^2} \tag{15.38}$$

where F is the interaction force and η the oil viscosity. Clearly as the attraction force increases as s decreases, the drop separation s decreases to zero in a finite time which gives an upper bound for the coalescence time. Let us consider the simplest case of two drops of radius R_0 between which a potential difference ΔV is maintained. A good approximation of the attraction force is [26]:

$$F = \frac{\pi}{2}\varepsilon(\Delta V)^2 \frac{R_0}{s} \tag{15.39}$$

The velocity of drop approach is then constant:

$$\frac{ds}{dt} = -\frac{1}{3}\frac{\varepsilon(\Delta V)^2}{\eta R_0} \tag{15.40}$$

Defining t_{ec} as the time necessary for the drop separation to pass from $R_0/3$ to zero we obtain:

$$t_{ec} = \frac{\eta R_0^2}{\varepsilon(\Delta V)^2} \tag{15.41}$$

A typical value is $t_{ec} \approx 50$ ms for $\Delta V/R_0 = 1$ kV/cm.

This picture of total film draining holds for rigid spheres of well-defined radius. This apparently excludes the cases where drops upon collision form flat channels, dimples, etc. However, the strong electrostatic pressure in the zone of small distance between droplets tends to keep the facing surfaces convex and very likely prevents the formation of flat channels or dimples. Moreover, the radii of curvature of the facing parts of the interfaces should tend to decrease which should help film draining and, hence, diminish the upper bound of coalescence time.

In the above scenario of film thinning, it was implicitly assumed that the parts of the drop surfaces subjected to strong electric forces keep their smooth shape. If we refer to the qualitatively

similar problem of disintegration of a single conducting drop in a uniform field, it is clear that the interfaces will destabilize when the effect of electrostatic pressure, inducing a deformation of the facing interfaces, overcomes the restoring action of surface tension. We can therefore give the following description of the process of electrocoalescence: after a first stage of approach of the two droplets resulting from the action of the shear (or of the electric field in a stagnant emulsion), there is a second stage of film thinning and drop deformation until the interfaces destabilize and lead to the generation of a bridge between the drops in a very short time. The instability development has not yet been investigated and characterized; from the study of single drop disintegration (see Section 15.5), and from recent observations, one can only infer that it is a very rapid process possibly involving the formation of a rather narrow jet. The conditions under which instability and coalescence set in are better delineated.

15.6.2 Critical Conditions

Several studies have focused on this question. Strictly speaking they do not concern the instability conditions but rather the determination of stationary solutions for two identical drops, the shape of which is distorted by the action of the electric forces. In these studies a dc applied field is assumed; the results also apply for ac sinusoidal fields provided that the frequency is very low and that the drops can be considered to be in quasi-static conditions at any time. The critical field $(E_0)_{\text{crit}}$ (or critical potential difference ΔV_{crit} between the drops) is determined as the maximum value beyond which a stationary solution no more exists.

The first study was performed in connection with raindrops in thunderstorms. Latham and Roxburgh [59] observed that drops placed not close to each other in an electric field would deform to ellipsoids and eventually disintegrate for high stresses. If the drops are very close, then coalescence would occur instead through an instability resulting in mass transfer from one drop to the other. Their derivation was based on the assumption of the drops taking an ellipsoidal shape and on the formulas of Davis [60] for the field value at the facing poles of spheres. They determined the critical value of the applied field as a function of the relative initial spacing s_0/R_0 of the drops and they found a fairly good agreement with their experimental measurements. A very interesting property can be derived from their results [61]: the critical separation s_{crit} is a fraction of the separation s_0 of the undistorted drops ($s_{\text{crit}} \cong 0.63 s_0$). This means that only a limited drop deformation is possible; beyond the critical deformation, the electrostatic pressure is higher than the capillary pressure and there is a dynamic process with the drop locally elongating until it reaches the other drop surface.

Taylor [62] considered the case of two closely spaced drops between which a potential difference ΔV is applied. The drops are anchored on two rings, which prevent them from moving toward each other. His main assumption was to consider that the spherical shape of the drops is distorted only in the zone delimited by the rings. Solving numerically the approximate equation for the deformed interfaces, he obtained predictions in good agreement with his experimental measurements. The most interesting results concern the asymptotic case of very small spacing of drops ($s_0/R_0 \ll 1$) characterized by the following critical conditions:

$$s_{\text{crit}} \cong \frac{1}{2} s_0 \qquad \Delta V_{\text{crit}} \approx 0.38 s_0 \sqrt{\frac{T}{\varepsilon R_0}} \tag{15.42}$$

Again static solutions exist only for a limited deformation correlated with a limited potential difference. An important point to be noted here is that the critical conditions correspond to a local field value in the oil film between the drops $\Delta V_{\text{crit}}/s_{\text{crit}}$ independent of the separation s_0.

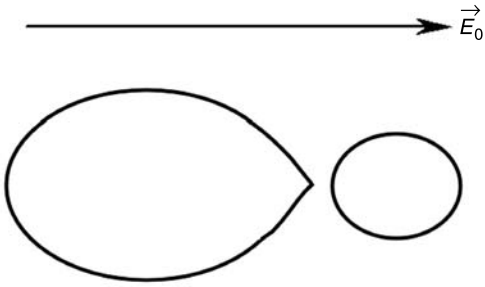

FIGURE 15.24 Deformation of close droplets.

Through a more sophisticated numerical treatment of the drop deformation problem, Brazier-Smith [63] confirmed that for $s_0 \ll R_0$ the surface distortion is mainly restricted to the zone where the drop surfaces are close (see Figure 15.24). By examining the time evolution of the drop shapes, it was shown [64] that for large enough drop separation ($s_0 > 1.2R_0$), like for a single drop, the instability occurs through the cone-jet mode. For smaller separations there is no evidence for a jet-like formation.

In the case of very small values of the distance s_0 between nondeformed drops, which is of interest for electrocoalescer applications, we propose a physical picture [61] which illustrates the phenomenon and justifies the laws obtained by Taylor. The drops are distorted only in the zones where the interfaces are at a short distance and where the electrostatic pressure p_{es} takes high values:

$$p_{es} = \frac{1}{2}\varepsilon E^2 = \frac{1}{2}\varepsilon \frac{\Delta V^2}{z^2} \tag{15.43}$$

By denoting s the separation between drops and by taking the following parabolic expression for the distance z between the interfaces at the radial distance r from the 2 drops axis:

$$z = s + \frac{r^2}{R_0} = s\left[1 + \frac{r^2}{R_0 s}\right] \tag{15.44}$$

we see that the electrostatic pressure distribution has a characteristic scale $(R_0 s)^{1/2}$. The distorted zone of the drops then has a radius $r_{dist} = A(R_0 s)^{1/2}$, A being a numerical constant (outside this region the drop deformation can be neglected). This is an asymptotic solution valid for $s/R_0 < 1/A^2$. Assuming that the centers of the spherical parts of the drops are immobile and that the deformed parts ($r \leq r_{dist}$) are characterized by a radius of curvature $R < R_0$, a simple relation between R and R_0 is deduced [61]:

$$\frac{1}{R} - \frac{1}{R_0} = \frac{1}{A^2}\frac{s_0 - s}{R_0 s} \tag{15.45}$$

where s_0 is the spacing between the undistorted drops. Balancing the capillary pressure difference between pole and spherical part and the electrostatic pressure at the poles leads to [61]:

$$(\Delta V)^2 = \frac{4}{A^2}\frac{T}{\varepsilon R_0} s(s_0 - s) \tag{15.46}$$

The maximum of ΔV gives the critical conditions:

$$\Delta V_{\text{crit}} = \frac{1}{\text{A}} s_0 \sqrt{\frac{T}{\varepsilon R_0}}, \quad s_{\text{crit}} = \frac{s_0}{2} \tag{15.47}$$

and we recover Equation 15.42 by taking $A \cong 2.6$. In the case of two drops subjected to a uniform field E_0, the main difficulty is to evaluate ΔV; using the asymptotic expression for ΔV valid for spheres (Equation 15.30), the following critical value for the field can be proposed:

$$(E_0)_{\text{crit}} \cong 0.058 \frac{s_0}{R_0} \log\left(\frac{2R_0}{s_0}\right) \sqrt{\frac{T}{\varepsilon R_0}} \tag{15.48}$$

This relation can also be used to determine the critical separation s_0 for a given applied field E_0.

All the investigations recalled here considered only two identical drops. In the case of drops of different radii, the biggest drop has the lowest internal pressure (due to surface tension) and its surface is more easily deformed. Therefore it is the interface of the biggest drop that will become unstable first (see Figure 15.24).

Up to now we have examined the case of dc applied field. Using an ac voltage of rectangular shape defines conditions for drop deformation fully equivalent to dc ones. With a sinusoidal applied voltage, the problem is different and it is not possible to take into account the effective applied field only. The electrostatic pressure has a mean value and a sinusoidal component at the doubled frequency. This periodic component induces a periodic modulation of the surface distortion whose amplitude and influence on the interface stability depend on frequency. The example of the disintegration of a single drop (see Section 15.5) illustrates such a role of frequency, which presumably should influence the critical conditions.

In the practical case of demulsification of crude oils, which contain numerous chemical components, the situation is not as ideal as hypothesized in the aforementioned studies. With surfactants the surface tension might vary with the interface deformation and expansion, which should drastically modify the conditions of electrocoalescence (for example naphthenic acids have a stabilizing effect on water-in-oil emulsions). In the case where the drops are covered with a surface film (like asphaltenes, bitumen, and resins) having a certain stiffness, the drop deformation is affected by this stiffness and the thinning of the coating layer might play the major role in controlling the coalescence process. Another phenomenon to take into account is the presence of particulate surface layers which would act as spacers maintaining the surfaces of close drops at a finite distance and thus hindering coalescence. In all these cases it is not possible to use the electrocoalescence conditions deduced from the analysis of the ideal case and, therefore, to design a "universal" electrocoalescer; the basic phenomena must be clearly characterized before attempting to derive critical conditions for electrocoalescence.

15.6.3 Experimental Investigations of Falling Drops

Contrary to many earlier investigations on basic phenomena of drop–drop electrocoalescence we have used ac fields. The influence of the shape, frequency, and magnitude of ac electric fields was studied in an optical bench under homogeneous field conditions described in Ref. 48. Furthermore, the influence of factors like salinity and surface-active substances has been studied.

The greater part of the experiments was done with one smaller drop falling on to a larger drop resting at the lower electrode. The stationary drop was either in direct contact with the electrode surface (non insulated drop), or separated from the electrode by a polypropylene disk (insulated drop). Observations were made with a fast (1000 fps full resolution) video camera. Under sinusoidal ac voltages we typically would see the lower surface (with lower curvature and internal pressure) starting to deform and oscillate with the applied field when the drop approached, and then starting to deform when the falling drop came close. When using square wave ac the oscillations disappeared. As water has a higher density than oil, the drop will fall down and after some time reach a terminal velocity, until it gets close to the surface of the lower drop where it is retarded by the film draining forces as shown in Figure 15.25.

Without an applied field the falling drop would generally roll off the larger drop (Figure 15.26). Applying an electric field will create a force that increases the velocity. For lower fields the falling droplet would now rest for some seconds at the summit of the lower one before coalescing, while for increasing fields a quick coalescence would occur. Even at 10^4 frames per second we could not resolve the final coalescence event. Often, after the collapse, a smaller satellite drop was pinched off from the larger drop, as seen from Figure 15.27(c).

A large number of experiments were done in order to study coalescence efficiency between drops that collide. A set-up like that shown in Figure 15.27(a) was used. The size of the falling

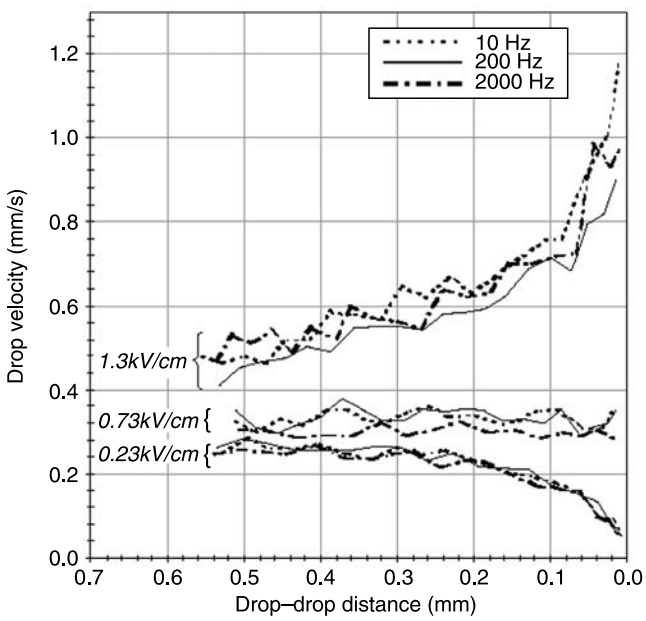

FIGURE 15.25 Velocity of the lower interface of a 200 μm drop as the drop falls on to the larger drop; influence of applied field and frequency. Square wave ac voltage.

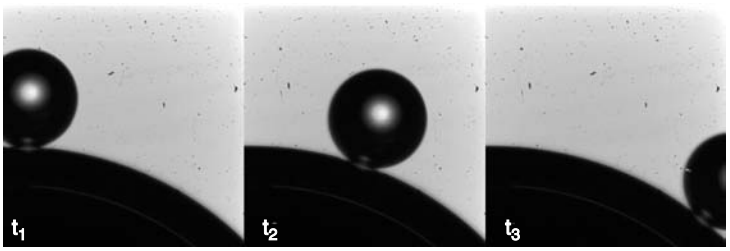

FIGURE 15.26 Drop impact at zero electric field with drop rolling off.

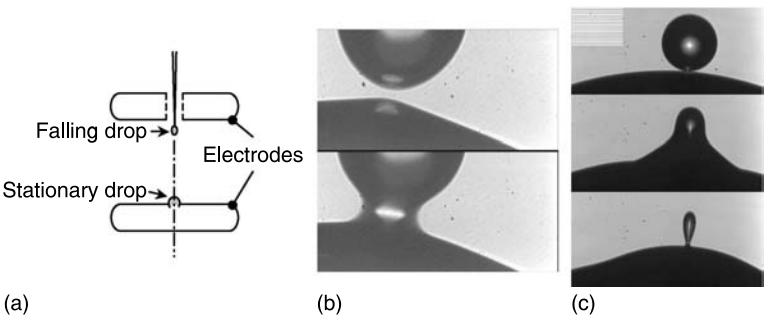

FIGURE 15.27 Experiments with falling drop: (a) Experimental set-up with small drops falling on a large drop at 3 to 4 kV/cm; (b) 90 μm drop falling and deformation of lower drop; and (c) 500 μm drop falling, coalescing, and forming a satellite drop.

drop was in the 200 μm range, and a square ac voltage with varying amplitude was used. The square voltage was used to avoid the more imprecise situation of a time variant force occurring under sine wave conditions. The time for drops to coalesce after they appeared to be in apparent contact was recorded. Then at higher stresses the coalescence would occur instantaneously when the drop hit or came so close that it looked like impact and at even higher stresses the coalescence would occur before the impact. Typical results are shown in Figure 15.28. Figure 15.28(a) suggests that we have two dependencies between time to coalesce: one for times above 0.05 sec where more than one half period is needed for coalescence to occur and one for shorter times where we are in the range where instantaneous coalescence occurs. At the present time we cannot explain the different results between isolated and non-isolated stationary drops.

In another experiment we found indications that for small diameter falling drops we had to go to higher fields, which is perfectly in line with the hypothesis that the instantaneous coalescence is governed by instability formation with a critical field that increases when size of the smaller drop is reduced. However, these results were obtained with sine voltage excitation, and therefore difficult to interpret.

15.6.4 Non-Ideal Surfaces

When the influence of asphaltenes was studied the water drops were kept for 20 min to allow saturation on their surfaces. Typical coalescence times are shown in Figure 15.28(b). The differences between oils with and without asphaltenes can be explained by the reduced interfacial

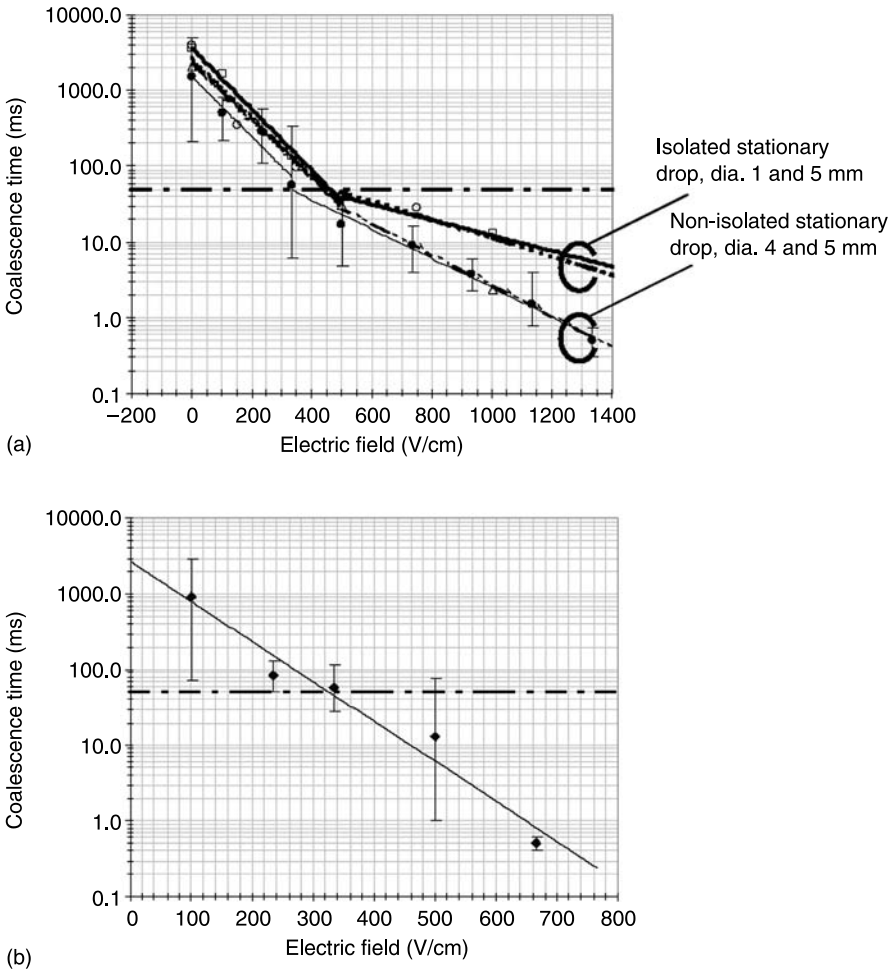

FIGURE 15.28 Coalescence time for water drops added 3.5 wt% NaCl in naphthenic oil under the influence of a 10 Hz square wave electric field. 200 μm falling drop. (a) Pure oil (no additives). A break in the curves occurs at 50 ms, corresponding to half the voltage period. (b) 100 ppm asphaltenes dissolved in oil phase. Saturated drop surfaces. Non-isolated, 4 mm stationary drop.

tension of the asphaltene oil. For oils with asphaltenes added the interfacial tension varied with time starting at 35 mN/m and falling towards 5 mN/m over a 20 min period, compared to the pure oil having a surface tension of 40 mN/m. One important difference between the pure oil and oil containing asphaltenes was that the voltage to get a coalescence time of 0.5 msec was reduced from 1350 V/cm to 700 V/cm. Another important difference was the time needed to drain the upper water drop once puncture of the surfaces was established. For the pure oil the drop collapsed within one millisecond, while for asphaltene saturated water drops the draining could take more than 1 min (see Figure 15.29). In the latter case no satellite was formed. This clearly shows the influence of the stiff surface layer. How such a stiff layer would influence

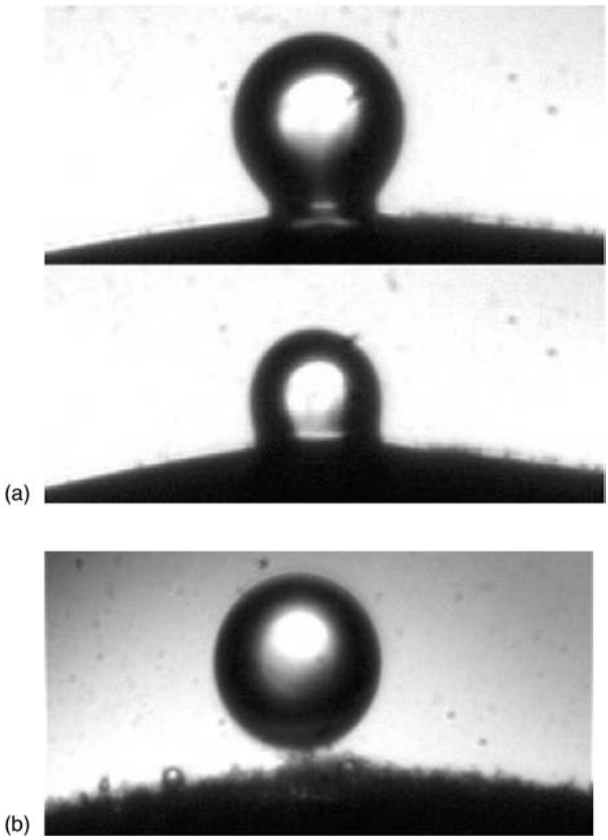

FIGURE 15.29 Surface covering. *Top* (a): Slow draining (>0.5 sec) of asphaltene covered coalesced drop. *Bottom* (b): Particulate maters preventing coalescence of a 200 μm droplet.

the formation of the instability cone remains unknown. However, our results indicate that the timescales for the instability formation are sub-millisecond in all cases.

For the experiments with asphaltenes the surface of the larger drop often got contaminated with small particles. These would tend to concentrate at the summit of the larger drop and could prevent coalescence, as shown in Figure 15.29.

Experiments in oils with asphaltenes added gave the same results for 10, 200, and 2000 Hz square wave voltage. This is in line with our theory that it is the level of the instantaneous field, and the dipole moment this field induces, that in the case of uncharged droplets govern the coalescence process.

15.6.5 Experiments with Supported Drops

As it is troublesome to do visual observations with moving drops, several experiments were done with drops fixed in various ways; hanging on capillaries or resting on PTFE surfaces as shown in Figure 15.30. These experiments often produced effects that could not be reproduced with free drops.

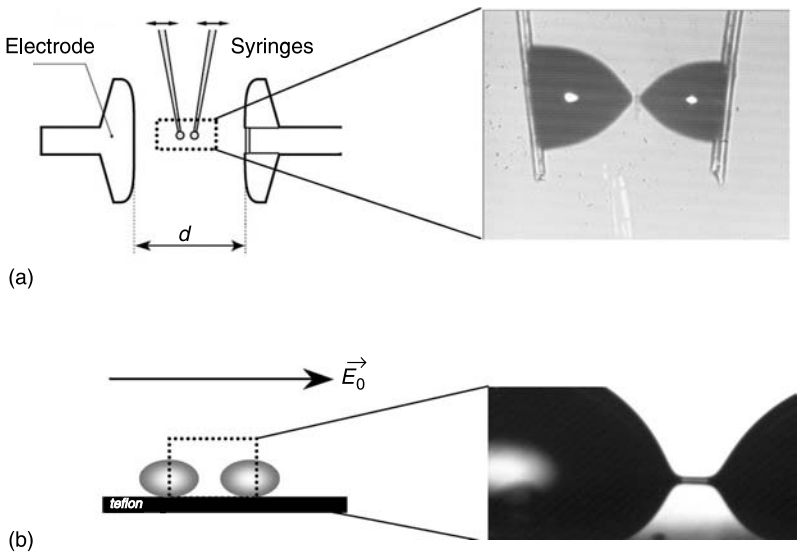

FIGURE 15.30 Non-coalescing drop pairs. Experiments with (a) drops hanging from glass capillaries and (b) drops resting on a Teflon surface.

With water filled glass capillaries we found that for low frequencies coalescence occurred at low background fields. With increased frequencies the field at which coalescence occurred increased until finally at 10 kHz we could get stable "instability cones" without coalescence occurring at all. The drops were not in contact with the water inside the capillary as seen from Figure 15.30(a). We explain the missing coalescence by a force due to the good capacitive coupling at higher frequencies between the water drop and the water column inside the capillary that "glued" the drops to the capillaries, and thereby preventing them to freely coalesce. Furthermore, the water jets from the capillaries hit each other with opposing direction.

Similar experiments were performed with drops resting on a horizontal Teflon surface. Small drop pairs became unstable and coalesced as expected, independent of the applied frequency in the range 10 Hz to 10 kHz. However, with large droplets (radius $\sim$ 1 mm) we could observe a stable channel forming between the two drops as shown in Figure 15.30(b). Apparently, again this was due to forces adhering the drop to the solid surface, thus preventing their mass centers to move.

Attempts to reproduce these effects for free drops and emulsions failed, and we conclude that one should be careful to extrapolate experiences with supported drops to real emulsions.

15.7 SOME CONSIDERATIONS REGARDING PRACTICAL ELECTROCOALESCERS

Possibly the largest problem for an oil/water separator, and also for an electrocoalescer, is to treat oils with a low water cut and small drops: Small drops gravitate slowly towards the bottom of a sedimentation tank, and the distances between drops will be considerable. The overall coalescence efficiency is given by the drop collision rate and the probability that the drops will coalesce once they are in close proximity to each other.

This far we have mainly looked at electrostatic forces on drops and drop pairs under stagnant or laminar flow conditions. This is relevant for the typical older generation electrocoalescers in large sedimentation tanks. However, during the last decade a new concept has arrived, where shear movement in the emulsion is applied to create more frequent drop collisions [9,26,65]. From an analysis of movement of drops suspended in liquids one may calculate the collision frequency. With this we do not mean direct impacts between drops, but situations where the drops gets close enough to allow the short range electrostatic forces to give a large enough force to pull them together. So "impact" is based on a criterion determined by when the drops come within a certain capture radius where the electrostatic attractive forces exceeds the viscous drag. Increasing turbulence and shear flow can increase this collision rate. The upper allowed limit of the turbulence is where it rips apart drops that get in proximity of each other, or even more extreme; results in drop fragmentation. An *efficient collision cross section* can be developed depending on drop size, electric field, and liquid shear movement.

Once the drops are within each other's efficient cross section, the achieved time to coalescence is reduced with increasing background fields as described in Figure 15.28. At a certain critical voltage and drop distance combination, instantaneous coalescence will occur. The coalescence efficiency can be increased by raising the field towards the limit where the larger drops in the emulsion start to become unstable.

The designer has, on the one hand, to balance shear flow (or turbulence) between high collision frequency between drops and ripping apart drop pairs or existing large drops. On the other hand, he has to balance the electric field between the need of getting large collision cross sections and high coalescence efficiency, and the danger of destroying large drops by initiating instabilities.

Our analysis points at electrostatic attractive forces and surface instability as being the governing factors for electrocoalescence. From this point of view a high dc field, where the driving field is continuously high, seems favorable. However, if covered electrodes are chosen in order to reduce the risk of breakdown from water plugs, this may result in a resistive voltage distribution. Then the solid, highly resistive dielectric barrier may take all the voltage leaving the emulsion as a low field region. The use of so-called pulsed dc, which has been suggested by several authors [66], is an attempt to solve this problem. During the voltage steps, the pulsed dc redistributes the field from a resistive to a capacitive distribution. Though after some time, which is given by the time constant of the emulsion, the distribution will fall back to the resistive mode, and a new voltage transient is needed. Transients therefore need to be applied with short intervals. However, if they become too short, the system will not get time to relax back to its initial state and the effect of the steps will be reduced. A better alternative is to use high frequency ac fields that distribute voltages capacitively all the time, giving increased fields in the emulsion compared to the low frequency or dc case. It is the net conductivity of the emulsion that determines how high a frequency is required, as described in Section 15.3.

For a drop pair, an ac field will, in general, result in a lower coalescence efficiency than a dc field, because during parts of the period the field will have fallen below the critical level; the duty cycle, being the percentage of time where the field is above the critical value, will be less than 100%. The duty cycle of a dc voltage is 100%. However, as explained above, dc can result in problems in coalescers with covered electrodes. To overcome this, one can use an ac square voltage. The forces will act equally efficiently as under dc field conditions, with a duty cycle of 100%. Increasing the field will also increase the duty cycle, but also stress the insulation system, which often is sensitive to the peak stress. The downside of using square ac voltages is that it will invoke some form of power electronics, which can be costly, while sine voltages are easily produced using a transformer.

There have been discussions about optimum frequencies for ac coalescers. It is difficult to imagine any "universal optimum." We would suggest that in the case of covered electrodes, as explained above, the main criterion is that the duration of one half period of the voltage should be short compared to the time constant of the oil, as explained in Section 15.3. For uncovered electrodes where the drops are charged at the electrode surfaces, under laminar flow or stagnant fluid condition, the drift velocity and the separation of the drops will be determining factors. When coalescence occurs between singular droplets and not at the electrode surfaces, it will mainly occur between oppositely charged drops. The drops must therefore be allowed to keep their acquired charge long enough to meet drops of opposite polarity. As drops lose charge with time as they propagate away from one electrode towards the opposite it could be advantageous to divide the electrode gaps into shorter gaps where less charge is lost. Additionally, it would be advantageous to have an inhomogeneous field that allows uncharged drops to be attracted to an electrode and become charged. One should also consider that in addition to the attractive or repulsive forces between charged drop pairs, the applied field will also act on each charged drop. As we observed in our emulsion experiments, the interaction with the applied field (Equation 15.1) can be stronger than between the drops (Equation 15.2).

We have this far mainly considered emulsions with a low water cut. The coalescer design will have to be adapted to the conditions of the particular oil reservoir as discussed by Tsabek [52], for example. For systems with high water cuts the drop–drop collisions become more frequent and chain formation more likely to occur. Forces that keep drop chains together are described in studies dealing with particle/oil suspensions used for rheological purposes [44].

In the production of crude oil, it is not only the emulsified water that is the problem; there are gases under varying pressures, and there may be sand particles and salts that must be removed by gas scrubbers, cyclones, sedimentation tanks etc. The sequence in which this equipment is assembled is not indifferent to the final result; e.g., if one at an early stage can remove smaller particles then particle stabilizing of the drop surfaces is less likely to occur in the electrocoalescer. This far the electrocoalescers have usually been combined with and built into the sedimentation tanks. It seems advantageous to apply a more compact unit in front of the sedimentation tank, taking advantage of the liquid mixing in the turbulent flow in pipelines before the sedimentation tank with a more stagnant condition. If drop sizes at the inlet can be increased, then the volume of the sedimentation tanks can be reduced. The effect of an experimental compact coalescer is shown in Figure 15.31.

Finally, one must not forget a possible influence of streaming electrification and triboelectric effects that may start to play a role at higher liquid velocities. Most scientific studies are done either as optical studies in stagnant emulsions or looking at drop size distributions for model systems with liquid flows. In these studies there is little support for hypotheses or conclusions on the significance of this aspect. However, charging of droplets occurred frequently in our experiments that mainly concerned forces on neutral, polarized drops and was a nuisance throughout our investigations. Most likely, charging will also occur in practical coalescers, but as time constants of the oil are small one would expect the effects to be limited. Still, this is an open question that should be further investigated.

ACKNOWLEDGMENTS

This work would not have been undertaken without the initial support from Statoil and ABB Offshore Systems (now Vetco Aibel) and the later substantial support from the Norwegian Research Council. We are most grateful to Pål Jahre Nilsen from ABB Offshore Systems in helping to start this project. We also acknowledge the assistance of Professor Johan Sjöblom in dealing

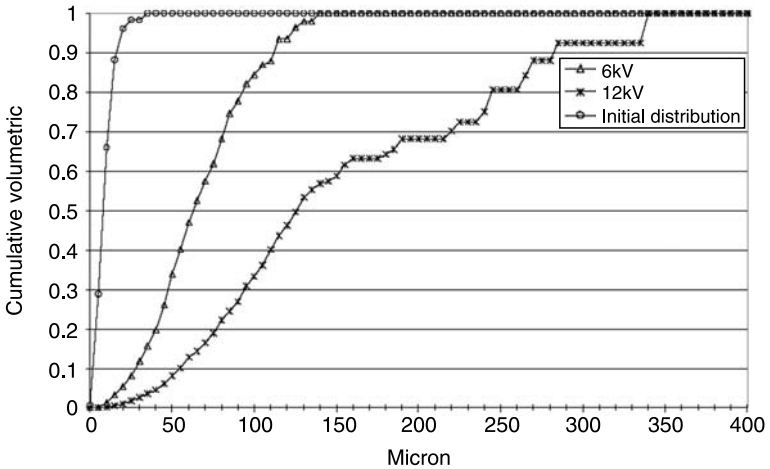

FIGURE 15.31 Cumulative water droplet size distribution in an emulsion treated with an electrostatic ac field. The emulsion flow has a Reynolds number of 20,000, and a residence time of 1 sec in the electric field. (Courtesy of Vetco Aibel.)

with the surface chemistry problems. The authors thank the International Electrotechnical Commission (IEC) for permission to reproduce figure 6 (page 40) from its International Standard IEC 60060-1(1989-11) 2nd edition — High-voltage test techniques. Part 1: General definitions and test requirements. All such extracts are copyright of IEC, Geneva, Switzerland. All rights reserved. Further information on the IEC is available from www.iec.ch. IEC has no responsibility for the placement and context in which the extracts and contents are reproduced by the author; nor is IEC in any way responsible for the other content or accuracy therein.

REFERENCES

1. E. Kuffel, W. S. Zaengl: "High Voltage Engineering", Pergamon Press, Oxford, 1988.
2. "Handbook of Electrostatics", Ed. J. Chang et al., Marcel Dekker, New York, 1995.
3. J. Cross: "Electrostatics: Principles, Problems and Application", Adam Hilger, Bristol, 1987.
4. F. G. Cottrell: "Breaking and separating oil water emulsions", US patent specification 895 729, 1908.
5. J. Sjöblom, N. Aske, I. H. Auflem, Ø. Brandal, T. E. Havre, Ø. Sæther, A. Westvik, E. E. Johnsen, H. Kallevik: "Our current understanding of water-in-crude oil emulsions. Recent characterization techniques and high pressure performance", Adv Colloid Interface Sci, 100–102 (Special Issue: A collection of invited papers in honour of Professor J. Th. G. Overbeek on the occasion of his 90th birthday), 2003, pp. 399–473.
6. L. C. Waterman: "Electrical coalescers", Chemical Engineering Progress, 61 (10), 1965, pp. 51–57.
7. J. S. Eow, M. Ghadiri, A. O. Sharif, T. Williams: "Electrostatic enhancement of coalescence of water droplets in oil: a review of the current understanding", Chem. Eng. J., 84 (3), 2001, pp. 173–192.
8. J. S. Eow, M. Ghadiri: "Electrostatic enhancement of coalescence of water droplets in oil: a review of the technology", Chem. Eng. J., 85, 2002, pp. 357–368.
9. O. Urdahl, N. J. Wayth, H. Førdedal, T. J. Williams, A. G. Bailey: "Compact Electrostatic Coalescer Technology", In: Encyclopedic Handbook of Emulsion Technology (Ed. J. Sjöblom), Marcel Dekker, 2001, pp. 679–694.

10. L. Onsager: "Deviation from Ohm's law in weak electrolytes", J. Chem. Phys., 2, 1934, pp. 599–615.
11. IEC publication IEC 60-1 (1989) High-voltage test techniques Part 1: General definitions and test requirements.
12. N. J. Felici: "Forces et charges de petits objets en contact avec une électrode affectée d'un champ électrique", Revue général de l'électricité, 75, 1966, pp. 1145–1160.
13. M. Zahn: "Space charge effects in dielectric liquids". In: The Liquid State and its Electrical Properties, Plenum Press, New York, 1988, pp. 367–430.
14. A. Pedersen, E. Ilstad, A. Nysveen: "Forces and movement of small water droplets in oil due to applied electric field", Conf. Proc. Nordic Insulation Symposium, NORD-IS, 2003, pp. 127–133.
15. C. Crowe, M. Sommerfeld, Y. Tsuji: "Multiphase flows with droplets and particles", 2nd edition, CRC Press, Boca Raton, 1998, ISBN 0-8493-94694.
16. D. M. LeVan: "Motion of droplets with a Newtonian interface", J. Colloid Interface Sci., 83, 1981, pp. 11–17.
17. J. A. Melheim, M. Chiesa, A. Pedersen: "Forces between two water droplets in oil under the influence of an electric field", 5th International Conference on Multiphase Flow, ICMF'04, Yokohama, Japan, May 30 to June 4, 2004, Paper No. 126.
18. D. J. Klingenberg, F. van Swol, C. F. Zukoski: "The small shear rate response of electrorheological suspensions. II. Extensions beyond the point-dipole limit", J. Chem. Phys., 94 (9), 1991, pp. 6170–6178.
19. H. J. H. Clercx, G. Bossis: "Many-body electrostatic interactions in electrorheological fluids", Phys. Rev. E, 48 (4), 1993, pp. 2721–2738.
20. K. W. Yu, T. K. Wan Jones: "Interparticle forces in polydisperse electrorheological fluids", Comput. Phys. Commun., 129, 2000, pp. 177–184.
21. Y. L. Siu, T. K. Wan Jones, K. W. Yu: "Interparticle force in polydisperse electrorheological fluid: Beyond the dipole approximation", Comput. Phys. Commun., 142, 2001, pp. 446–452.
22. P. M. Morse, H. Feshbach: "Methods of Theoretical Physics, Part II", McGraw-Hill, New York, 1953.
23. G. W. Carter, S. C. Loh: "The Calculation of the Electric Field in a Sphere-gap by Means of Dipolar Co-ordinates", IEE Monograph, No. 325 M, pp. 108–111, 1959.
24. M. H. Davis: "The Forces Between Conducting Spheres in a Uniform Electric Field", RM-2707-1-PR, Rand Corporation, 1962.
25. M. H. Davis: "Two Charged Spherical Conductors in a Uniform Electric Field: Forces and Field Strength", RM-3860-PR, Rand Corporation, 1964.
26. P. Atten: "Electrocoalescence of water droplets in an insulating liquid", Journal of Electrostatics, 30, 1993, pp. 259–270.
27. T. J. Williams, "The resolution of water-in-oil emulsions by the application of an external electric field", PhD Thesis, Univ. Southampton, UK, 1989.
28. A. Pedersen, E. Ilstad, A. Nysveen: "Forces and movement of water droplets in oil caused by applied electric field", IEEE Conference on Electrical Insulation and Dielectric Phenomena, Colorado, USA, 2004.
29. K. Adamiak: "Force of attraction between two conducting droplets in electric field", Proceedings of the 1999 IEEE Industry Applications Society Annual Meeting, Phoenix, Arizona, Vol. 3, 1999, pp. 1795–1800.
30. K. Adamiak: "Interaction of two dielectric or conducting droplets aligned in the uniform electric field", Journal of Electrostatics, 51–52, 2001, pp. 578–584.
31. R. H. Davis, J. A. Schonberg, J. M. Rallison: "The lubrication force between two viscous drops", Phys. Fluids A, 1 (1), 1989, pp. 77–81.
32. O. I. Vinogradova: "Drainage of a thin liquid film confined between hydrophobic surfaces", Langmuir, 11, 1995, pp. 2213–2220.
33. G. Barnocky, R. H. Davis: "The lubrication force between spherical drops, bubbles and rigid particles in a viscous fluid", Int. J. Multiphase Flow, 15, 1989, pp. 627–638.
34. D. J. Klingenberg, F. van Swol, C. F. Zukoski: "Dynamic simulation of electrorheological suspensions", J. Chem. Phys., 91, 1989, pp. 7888–7895.

35. I. V. Lindell, G. Dassios, K. I. Nikonskinen: "Electrostatic image theory for the conducting prolate spheroid", J. Phys. D: Appl. Phys., 34, 2001, pp. 2302–2307.
36. R. T. Bonnecaze, J. F. Brady: "Dynamic simulation of an electrorheological fluid", J. Chem. Phys., 96, 1992, pp. 2183–2202, 1992.
37. T. B. Jones: "Forces and torques on conducting particle chains", Journal of Electrostatics, 21, 1988, pp. 121–134.
38. T. B. Jones: "Dipole moments of conducting particle chains", J. Appl. Phys., 60, 1986, pp. 2226–2230.
39. T. B. Jones: "Effective dipole moment of intersecting conducting spheres", J. Appl. Phys., 62, 1987, pp. 362–365.
40. I. V. Lindell, J. C. E. Sten, K. I. Nikonskinen: "Electrostatic image method for the interaction of two dielectric spheres", Radio Science, 28, 1993, pp. 319–329.
41. J. C. E. Sten, K. I. Nikoskinen: "Image polarization and dipole moment of a cluster of two similar conducting spheres", Journal of Electrostatics, 35, 1995, pp. 267–277.
42. E. v. d. Bosch: "Electrostatic coalescence and light scattering", PhD Thesis, TU Eindhoven, Netherlands, 1996. ISBN 90-386-0179-4.
43. J. A. Melheim: "Cluster integration method for Lagrangian particle dynamics", *Comput. Phys. Comun.*, 171(3), 2005, pp. 155–161.
44. P. Atten, P. Gonon, J.-N. Foulc, C. Boissy: "Estimate of the electric stress in the liquid lying between particles of an electrorheological fluid", 1999 IEEE Conf. El. Ins. and Diel. Phenomena, pp. 333–336.
45. P. Atten, C. Boissy, J.-N. Foulc: "Slightly conducting spheres immersed in a dielectric liquid subjected to a DC field: attraction force, electric field on the liquid and partial discharges", Proc. 13th Intl. Conf. Diel. Liquids, ICDL, Japan, 1999, p. 111.
46. R. T. Bonnecaze, J. F. Brady: "Dynamic simulation of an electrorheological fluid", J. Chem. Phys., 96, 1992, pp. 2183–2202.
47. L. C. Davis: "Polarization forces and conductivity effects in electrorheological fluids", J. Appl. Phys., 72, 1992, pp. 1334–1340.
48. L. Lundgaard, G. Berg, A. Pedersen, P. J. Nielsen: "Electrocoalescence of water drop pairs in oil", Proc. 14th Int. Conf. on Dielectric Liquids, ICDL, Austria, 2002, pp. 215–219. ISBN 0-7803-7350-2.
49. C. T. R. Wilson, G. I. Taylor: Proc. Camb. Phil. Soc. 22, 1925, p. 728.
50. G. I. Taylor: "Disintegration of water droplets in an electric field", Proc. R. Soc., London, A 146, 1964, pp. 383–397.
51. J. D. Sherwood: "Breakup of fluid droplets in electric and magnetic fields", J. Fluid Mech., 188, 1988, pp. 133–146.
52. L. K. Tsabek, G. M. Panchenkov, V. V. Papco: "Theoretical basis of operation of equipment for electrical dehydration and electrical desalting of oil emulsions", Special paper no. 7, 8th Petroleum World Congress, Moscow, 1971, pp. 423–430.
53. G. Berg, L. Lundgaard, M. Becidan, R. S. Sigmond: "Instability of electrically stressed water drops in oil", IEEE ICDL 2002, Conference Record, Graz, 2004, pp. 220–224. ISBN 0-7803-7350-2.
54. S. B. Sample, B. Raghupaty, C. D. Hendricks: "Quiscent distortion and resonant oscillations of a liquid drop in an electric field", Int. J. Engn. Sci., 8, 1970, pp. 97–109.
55. R. Myrvold and F. K. Hansen: "Surface elasticity and viscosity from oscillating bubbles measured by automatic axisymmetric drop shape analysis", Journal of Colloid and Interface Science, 207, 1998, pp. 97–105.
56. T. Frømyr, F. K. Hansen, A. Kotzev, A. Laschewsky: "Adsorption and surface elastic properties of corresponding fluorinated and nonfluorinated cationic polymer films measured by drop shape analysis", Langmuir, 17, 2001, pp. 5256–5264.
57. C. W. Angle: "Chemical demulsification of stable crude oils and bitumen emulsions in petroleum recovery – a review". In: Encyclopedic Handbook of Emulsion Technology, Ed J. Sjöblom, Marcel Dekker, NY, 2001, pp. 541–594.
58. R. S. Allan, S. G. Mason: "Particle motions in sheared suspensions. XIV. Coalescence of liquid drops in electric and shear fields", J. Colloid Sci., 17, 1962, p. 383–408.

59. J. Latham, I. W. Roxburgh: "Disintegration of pairs of water drops in an electric field", Proc. Royal Soc., London, A295, 1966, pp. 84–97.
60. M. H. Davis: "Two charged spherical conductors in a uniform electric field: Forces and field strength", Quart. J. Mech. Appl. Math., 17, 1964, pp. 499–510.
61. P. Atten, L. Lundgaard, G. Berg: "A simplified model of electrocoalescence of two close water droplets in oil", Proceed. 5th Intern. EHD Workshop, Poitiers, 2004, pp. 119–123.
62. G. I. Taylor: "The coalescence of closely spaced drops when they are at different potentials", Proc Royal Soc. A, London, 306, 1968, pp. 423–434.
63. P. R. Brazier-Smith: "Stability and shape of isolated and pairs of water drops in an electric field", Physics of Fluids, 14 (1), 1971, pp. 1–6.
64. P. R. Brazier-Smith, S. G. Jennings, J. Latham: "An investigation of the behavior of drops and drop pairs subjected to strong electrical forces", Proc. Royal Soc. A, London, 325, 1971, pp. 363–376.
65. O. Urdahl, T. J. Williams, A. G. Bailey, M. T. Thew: "Electrostatic destabilisation of water-in-oil emulsions under conditions of turbulent flow, IChemE, 74 (part A), 1996, pp. 158–165.
66. P. J. Bailes, S. K. L. Larkai: "Liquid phase separation in pulsed dc fields", Trans IChemE, 60, 1982, pp. 115–121.